Design and Analysis of a Novel Artificial Cervical Disc

Zummurd Atef Mohammed Al Mahmoud

Submitted to the
Institute of Graduate Studies and Research
in partial fulfillment of the requirements for the degree of

Master of Science
in
Mechanical Engineering

Eastern Mediterranean University
January 2019
Gazimağusa, North Cyprus

Approval of the Institute of Graduate Studies and Research

Assoc. Prof. Dr. Ali Hakan Ulusoy
Acting Director

I certify that this thesis satisfies all the requirements as a thesis for the degree of Master of Science in Mechanical Engineering.

Assoc. Prof. Dr. Hasan Hacişevki
Chair, Department of Mechanical Engineering

We certify that we have read this thesis and that in our opinion it is fully adequate in scope and quality as a thesis for the degree of Master of Science in Mechanical Engineering.

Assoc. Prof. Dr. Neriman Özada
Supervisor

Examining Committee

1. Assoc. Prof. Dr. Neriman Özada
2. Asst. Prof. Dr. Mohammed Bsher A. Asmael
3. Asst. Prof. Dr. Ali Evcil

ABSTRACT

Artificial cervical disc plays a major role in implant surgeries, where it may work as much as the anatomical cervical disc after the replacement surgery. Therefore, designing and analyzing an artificial cervical disc became the main focus of this study. The Finite Element (FE) method was used to develop the design of artificial cervical disc between the cervical vertebra C4-C5 and to provide accurate analysis by using ABAQUS® software to determine the artificial disc response under static and dynamic loadings. The artificial cervical disc material was chosen from advanced biomaterials such as Cobalt Chrome Molybdenum (CoCrMo) and Ultra High Molecule Weight of Polyethylene (UHMWPE). Stress-strain relation, force displacement and compression were investigated under axial quasi static loading. Furthermore, in order to examine the model Range of Motion (ROM) in (axial rotation, lateral bending, and flexion/extension) moment was applied in three different directions. Moreover, another key analysis was normal mode of vibration, where, steady state dynamic and tabular amplitude was applied to investigate the effect of car accident on the artificial disc. In view of results, the maximum stress deformation was at the outer upper layer of CoCrMo, the yield strength was recorded as 170 MPa, the plastic deformation started at strain of 0.0005. As well as the failure occurs at 0.004. Coupled with displacement force distribution, the maximum deformation was in Z-direction. The moment load results showed the ROM of 5.36° and 5.89° in Flexion/extension, 7^olateral bending, and 6.7 ° axial rotations under 1000 Nmm. To enhance this work, results was validated by comparing with experimental and FE based data. Dynamic analysis showed that lower frequency may have more dangerous effect than higher frequency on ligaments. Nonetheless, maximum stress with 1.975e3 MPa at the upper layer of CoCrMo provided that tabular amplitude is applied. This work presented that the newly designed artificial disc is validation based on the comparison with previously published work.

Keywords: Cervical Disc, Artificial Disc, FE method, Static analysis, Range of motion, Dynamic analysis.

ÖZ

Yapay servikal disk protezinin, ameliyattan sonra anatomik servikal diske yakın hareket etmesi beklenmektedir. Bu nedenle, yapay bir servikal disk tasarlamak ve analiz etmek bu çalışmanın ana odağı olmuştur. Bu çalışmada, Sonlu Elemanlar (FE) yöntemi kullanılmış ve servikal vertebra C4-C5 arasındaki tasarlanan yapay servikal diskin statik ve dinamik yükler altındaki tepkisini belirlemek için ABAQUS® yazılımını kullanılmıştır. Yapay servikal disk malzemesi, Kobalt Krom Molibden (CoCrMo) ve Ultra Yüksek Molekül Polietilen Ağırlığı olan (UHMWPE) ileri biyomalzemelerden seçilmiştir. Eksenel yarı statik yükleme altında gerilme-gerinme ilişkisi, kuvvet yer değiştirmesi ve sıkıştırma incelenmiştir. Ayrıca, Hareket Aralığı modelini (ROM) incelemek için (eksenel dönüş, yanal bükülme ve bükülme / uzama) üç farklı yönde moment uygulanmıştır. Bu çalışmadaki bir diğer önemli analiz, normal titreşim moduydu. Burada araba kazasının yapay disk üzerindeki etkisini araştırmak için sabit durumlu dinamik ve tabular genlik uygulandı. Sonuçlar göz önüne alındığında, maksimum stres deformasyonu CoCrMo'un dış üst katmanındaydı, ve akma dayanımı 170 MPa olarak kaydedildi. Maksimum deformasyon z yönünde olmuştur. Moment sonuçları, Flexion /ekstansiyonda 5.36 ° ve 5.89 °, 1000 Nmm altında 7º tek bükülme, ve 6.7 º eksenel dönüş göstermiştir. Bu çalışmadan çıkan sonuçlar, deneysel ve Sonlu elemanlar bazlı verilerle karşılaştırılarak doğrulanmıştır. Dinamik analiz, düşük frekansın anatomik bağlar üzerindeki yüksek frekanstan daha tehlikeli etkiye sahip olabileceğini göstermiştir. Bununla birlikte, CoCrMo'un üst katmanında 1.975e3 MPa ile maksimum stres bulunmuştur. Bu çalışma yeni tasarlanan yapay disk`in daha önce yayınlanmış

çalışmalarla karşılaştırıldığında, diger çalışmalardaki yapay disklerle benzer sonuçlar verdigi doğrulanmıştır.

Anahtar Kelimeler: Servikal Disk, Yapay Disk, FE yöntemi, Statik analiz, Hareket aralığı, Dinamik analiz.

ACKNOWLEDGMENT

Foremost, I would like to express my sincere gratitude to my supervisor, Assoc. Prof, Dr. Neriman Ozada for the continuous support during MSc. study for her patience, support, motivation and for being there whenever I needed help.

I also like to thank my mother, for her invaluable support. I could not have being hear without her continues support and encourage.

TABLE OF CONTENTS

LIST OF TABLES

LIST OF FIGURES

LIST OF ABBREVIATIONS

ACDF	Anterior Cervical Discectomy
AF	Annulas Fibrosus
ASD	Adjacent Segment Disease
CEP	Cartilaginous endplates
CD	Cervical Disc
CTDR	Cervical Total Disc Replacement
DDD	Degenerative Disc Disease
FDA	Food and Drug Administration
FE	Finite Element
FEA	Finite Element Analysis
IVD	Intervertebral Disc
NDI	Neck Disability Index
NP	Nucleus Puposus
ROM	Range of Motion
UHMWP	Ultra High Molecule Weight of Polyethylene
VAS	Visual Analog Scale

Chapter 1

INTRODUCTION

1.1 Cervical Vertebra Problems and Medical Treatments

Cervical Vertebrae plays important roles in the human spine where it's the main structure of the neck and can be located immediately beneath the skull. It is one of the most complex structures in the human spinal. A high degree of movement and flexibility is possible to the large ROM required by the head [1]. Figure 1 shows the neck movements [2].

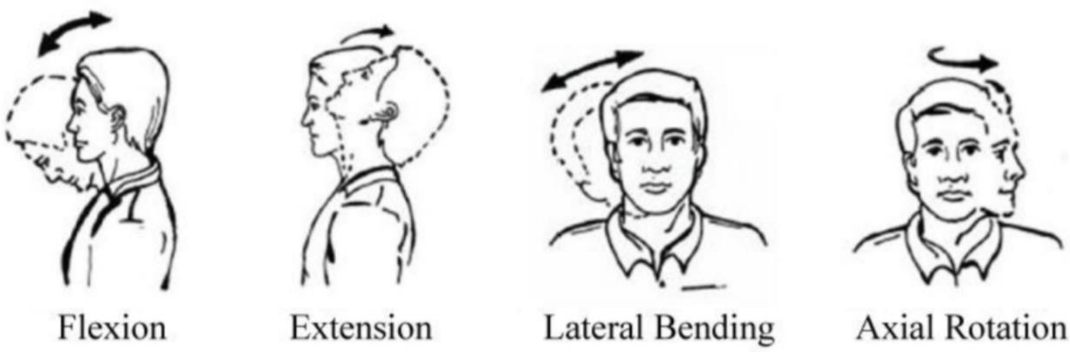

Figure 1: Neck movements

Cervical disc disease is caused due to irregularity in one or more of the discs that play the crucial role of 'cushions' that can be located between the neck bones (vertebra). Vertebral discs consist of three main components: nucleus puposus (NP), annulus fibrosus (AF), and cartilaginous endplates (CEP), providing the ability to distribute compressive load on adjacent vertebral bodies. Simultaneously, it also allows the vertebral column to bend and twist [3, 4]. Spinal movement has a certain level of restriction, in order to prevent injuries by the ligaments and facet joints [5].

Cervical vertebra is made up of unique features. The main function of each vertebra is to support the head while simultaneously restricting the head movements, in order to provide the essential level of protection to the spinal cord. The vertebral body is the largest bone section in the human body, as the external and cancellous bone located beneath which are the vertebras. Figure 2 present neck cervical vertebra and cervical disc clearly [6].

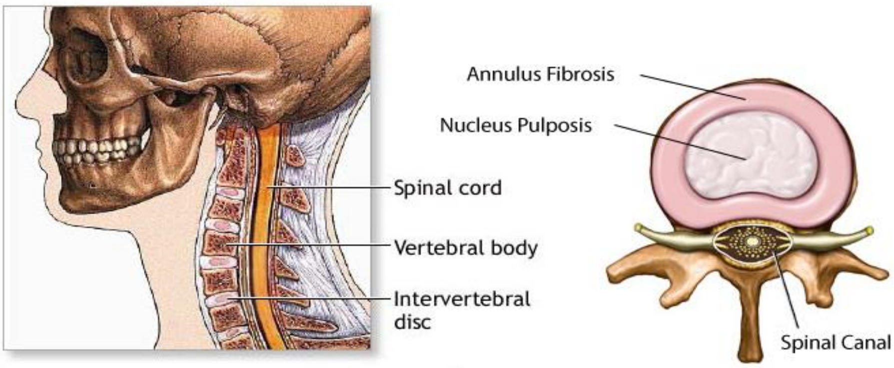

Figure 2: Cervical vertebra and cervical disc

Degeneration and disc herniation are major cervical disc (CD) problem. A multitude of causes of such problems can be defined as; 1) lifestyle habits, 2) different types of accidents, 3) Genetic abnormalities, 4) unhealthily safety environment and 5) Aging. Cervical vertebra and intervertebral disc (IVD) problems are known as the major causes of neck, shoulders and hand pain [7]. The most common symptoms are; 1) Neck stiffness and pain, 2) Pain in the shoulder and arm and 3) numbness in severe cases.

Recently, it has been notice that there has been an increase in interest of medical treatment that can be administered for such cases, in an effort to find the most efficient and more applicable solution for cervical disc and cervical vertebra problems. The following treatment methods can be used; 1) pain relievers, 2) physical therapy, 3) neck traction and 4) surgery by adding or replacing the damaged part with artificial cervical disc or adding a cage with a screw to stabilize the vertebra. Surgical intervention is the last option if any other treatment fails to alleviate the pain experienced by the patient. With today's medical abilities; Anterior Cervical Discectomy and Fusion (ACDF) is maintained as the conclusive surgical treatment for single and multi-level cervical degenerative disc disease (DDD) [8]. As an example of artificial cervical disc, (Prestige LP) artificial disc is produced by Medtronic. This disc has been used recently, in surgery where it is placed between the vertebrae's of issue, replacing the damaged discs. This artificial disc consists of two components, and the components are made up of a mixture of metals, including; titanium ceramic composite, and titanium carbide. Despite its artificial design, it has the same mobility of a natural disc, thus allowing the correct level of mobility to the neck, in terms of flexion/extension, bending, and rotation. Furthermore, it can be said that artificial cervical disc replacement assists in the reconstruction of regular motion, and it is a superior alternative of the current fuse surgery [9].

Not to mention, surgical management of CD has displayed vast progress especially during the last number of decades. This being the case, a multitude of surgical options for cervical vertebra damage can be located, providing a surgical solution for each patient with differing medical needs in this problem area.

1.2 Joints

Joints are one of the most important parts in human body, where it’s indicating the part of the body where the ends of two separate bones are connected together. Moreover, joints are the part that allows the movement of our skeleton and control the range of motion at the same time; likewise it controls the stability of the human skeleton. Where cervical vertebrae’s by itself can be defined as a joint, it is also made up of a structure of several types of joints. There are; atlanto-axial joint, facet joint at the back side of each vertebra and pivot joint. Additional to the above, there are also six different types of joints which are named: 1) hinge (it is the largest joint and it is the knee joint), 2) saddle, 3) plane, 4) condyloid, 5) ball-and-socket, and 6) fibrous. These allow required special movements and any differences between them can be seen in their structure and their shapes. In addition to this, lubrication fluid named synovial fluid can be located inside joints. Collagen fiber is the main component of fibrous joints. In cartilaginous joints, cartilage works to bind and connect bones to one another.

1.3 Cervical Vertebra Modeling and Analysis

From a kinematical point of view, the cervical spine is defined as a very complex structure, consisting of seven cervical vertebrae; it embodies a unique anatomy and a plethora of motion to accommodate the needs of a highly mobile head-torso transitory. Cervical motion is managed by anatomic restraints that protect the spinal cord and the connecting vascular structure. The cervical spine plays a supportive role in head movement and orientation in the three-dimensional space. Any disturbance to the anatomy or its mechanical properties may lead to clinical symptoms; as mentioned previously in Section 1.1. Age-related changes may modify the cervical anatomy, thus drastically reducing the alignment.

Due to the internal response of such a study, it is unsuitable for data to be collected via in-vivo or in-vitro studies only. Because of this issue, a need for a more developed technique arose. This resulted in the formation of Finite Element [10]. Finite Element assists in studying the biomechanical component of this complex structure, another key thing to remember dealing with the nonlinearity part of the structure. FE offers a vast variety in the definition of materials and their behavior. It additionally has the capability to analyze different mathematical models and engineering problems. Coupled with, some of the FEA commercial software can optimize the designs easily capturing the behavior of cervical vertebrae is vital for finite element simulation (FE), as the development of detailed FE models require accurate modeling of ligaments, cervical vertebrae, and disc and their mechanical properties.

The accurate analysis can be done by using modern software such as ABAQUS (Dassault Systèmes Simulia Corp). One of the most important stages in FEA is choosing element type and mesh size. When dealing with dynamic analysis, the density of the material should be defined in the section of material definition. However, if the analysis were to cover static analysis; it is only required to give the value of Young's Modulus and Poisson ratio. In general the materials used are consistent with the flexibility of elastic and are defined as isotropic material. In order to guarantee accurate results, the vertebral model should have symmetry, and the applied load case in both static and dynamic analysis should be realistic to nature. As a good result of accurate FEA data may reflect the same behavior of human cervical vertebra.

This study focuses on understanding the behavior of the artificial cervical disc ACD under static and dynamic loading, which is built on a nonlinear mathematical equation, to study the complex structure of the ACD. The finding can also be used in the future to evaluate impact loads and to study problems such as stress strain failure.

By using the FE method it is required to have a source of geometry of cervical vertebrae. This need was met with the volunteering of a female aged 24 years to contribute to this study. With her permission X-RAY photos were taken of her neck and shown in Figures 3 and 4 not to mention, there is a diverse amount of different biomaterials that may be used to design an artificial cervical disc. The materials that are the most commonly used can be listed as; titanium (Ti-6Al-4V), stainless steel (316 stainless steel) and cobalt chrome molybdenum (CoCrMo).

Figure 3: Right lateral view of neck

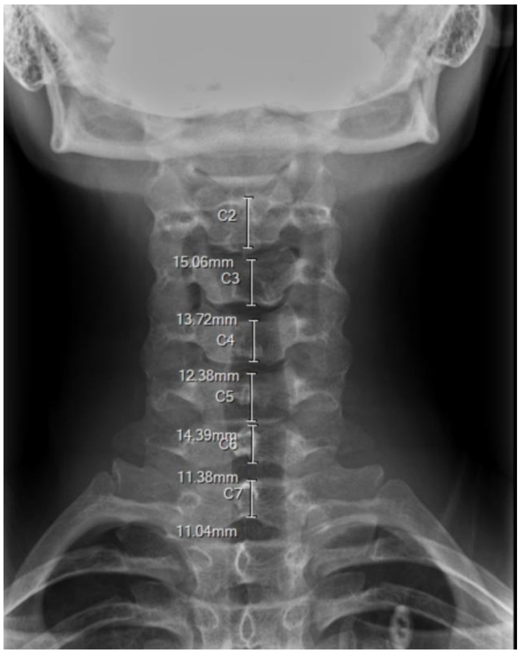

Figure 4: Anterior view of neck

A labeled section of cervical spine is shown in Figure 3 displaying an X-RAY of the right lateral side, while Figure 4 presents an X-RAY of the anterior.

Available artificial cervical disc device can be classified into two main categories; 1) total disc replacement (CTDR) 2) Anterior Cervical Discectomy and Fusion (ACDF). In the first case, only the nucleus (center of the disc) is replaced. In the second case the entire disc is removed and replaced by bone graft and installation by using screw.

1.4 Complications and Problems of Cervical Vertebrae after Treatment

Modern science and medicine are constantly developing in all areas of practice to improve previous techniques. Recent solutions may also cause some problems. It has been noted that on occasions where the physical therapy procedures have not been applied correctly, the injury has been increased.

Previous studies have reported positive results displaying treatment in some cases that have concluded with no additional problems, with patients returning to their daily life and activities as normal soon after [11]. Where minimally invasive surgical procedures can be used, an endoscopy is arguably the best approach for treating patients, especially young adults. Intrusive anterior methodologies are valuable procedures in terms of the treatment of cervical radiculopathy through a transuncal approach [12]. To that end, valuable such as; cases where problems occur post-surgery are evident. Among the problems exhibited is some cases is where the artificial plate may be swallowing, causing difficulty in breathing. In more severe cases, problems in relation to blood being pressured in to the head compressing the veins and causing swelling in the head have been noted. While a rare symptom;

patients may experience numbness and weakness in the arms. Another negative outcome may be the experiencing of a reaction to the medication. In some cases of neck pain, exercise and therapy may be preferred over surgery.

Most cervical disc pain can be reduced by conservative care and most cervical spine conditions can be improved. With positive collaboration between patients and their consultants, the likelihood of future problems can be decreased, preventing any advancement of degeneration and decreasing the chances of any relapses or flare-ups, thus is stopping the development of chronic pain syndromes [13].

It should be noted that in cases of the replacement of damaged discs with artificial cervical disc via surgery, (Presting LP cervical disc), due to the artificial disc being placed in such close proximity to nerves and blood vessels, there is a risk such major surgery could damage nerves and blood vessels, which in turn could lead to a large loss of blood and could be fatal.

1.5 Objective of the Thesis

The objective of this study is to design an artificial cervical disc, for the single level (C4 – C5), defining the most appropriate material, while taking in to consideration material properties and geometry for suitability between the vertebral and in accordance to the human anatomy are the part of the purpose. The second objective is to evaluate the maximum stress-strain under static axial load. Third objective is to find the ROM in different moment direction. The fourth objective is detection the effect of dynamic load on artificial cervical disc (ACD). Finally, it is aimed to compare the findings with published data.

1.6 Organization of the Thesis

This thesis provides general information about the field in Chapter 1introduction, including a definition and discussion of medical treatments, with also brief introduction to modeling and analysis and an initial idea in to what complications and problems following treatment may occur. Additional to the Introduction, a literature review is present within Chapter 2, displaying State of the Art options in Orthopedic and Medical Treatments, with a focus on radiography treatment, electromyography (EMG) and biomaterial and implements. Developments in joint modeling and analysis, especially the most recent developments focus on improving the patient's life post medical treatment. It covers a variety of development in cervical disc modeling and analysis. Raising the important issue of follow up with patients after surgical artificial cervical replacement's discussion in relation to studies focusing on improving the patient conditions after medical treatments with modern technology was presented along with the latest artificial disc devices, such as; Bryan device, ADCF , TDR-C, Bristol artificial disc, ProDisc-C Disc Prosthesis and other cases of cervical degeneration. At the end of chapter 2, the contributions of the current research are clarified.

Chapter 3 presents the theory and analysis of the study, outlining the steps of cervical vertebrae modeling and artificial disc modeling clearly, including it is geometry and take into consideration choosing the most applicable material, and definition with the mechanical properties and material behavior. Furthermore, Continuum mechanics and the fundamental equations which are used in FE analysis were explained. FE analyses, from the first step of defining the material to the last step of analysis, the details were clearly explained.

Chapter 4 provides the results for each analysis run separately and provide detailed results and their comparison with previously published works with discussion. Chapter 5 provides the conclusion and the future works of this study.

Chapter 2

LITERATURE REVIEW

2.1 State of the Art in Orthopedic and Medical Treatments

During the mid-nineteenth Century, Gwendoline Hunt and Albin Lambotte utilized stainless steel in the design of an implant created for fracture plate. Several years later; vanadium-iron was the preferred material over stainless steel, due to elastic nature. In the search for more biological implants; CoCrMo was suggested by AdalbertZierold [14]. In 1891, Plaster of Paires, ivory nickel plated screws and glue were used in the first hip replacement. In the beginning of 1940s, CoCrMo (specifically Vitallium) was used in the first replacement of a metal hip. A few years later in the year of 1952; the modern hip implant which is still in use until today was first developed. Ten years later; between 1962 and 1963, the modern total hip replacement was seen [15].What's more; a ductile ceramic bone was used to replace a patient's knee joint. The ductile ceramic bone, it was found, has almost the same physical properties of the knee bone, due to its make-up of 48% porosity and 11 Psi of flexural strength [16]. Few years later, in 1970; the complete knee arthroplasty was developed [17]. Over decades, since the first development of the hip and knee joint replacements, a dramatic increase in different types of prostheses has been observed [18]. 1964 was a remarkable year for cervical prosthesis, as the use of stainless steel the only published reported was documented by Reitz and Fernstrom. A few years later, the Bristol disc was designed with stainless steel as the material to construct the design for the second time. The ball-socket design has structure of metal on metal and connected to the vertebral by screw [19]. One of the disadvantages observed with this device its restriction in one size only, meaning it was not compatible with all anatomies. With the development of technology and material science, today it can be note that availability of new materials have drastically increase. However, biocompatible materials, .i.e., Ti, CoCrMo, and stainless steel are still in use. Generally, vertebral bone is encouraged to grow by making small cuts into it during artificial cervical disc replacement surgery [20, 21]

2.1.1 Radiography Treatment

In terms of radiography, the Micron-scale computed tomography (micro-CT) is deemed as necessary for phenol typing and elucidating diseases and their therapies. Throughout the last decades, this form of tomography has become more widely available, and has proved beneficial with its number of different applications. When comparing micro-CT with other instruments, it is notable as the best in high resolution and displays high efficiency while being less expensive. Micro-CT applications can be used for orthopedic imaging, where it may help in cervical spine imaging, as well as other areas such as cancer imaging in the lung and cardiac imaging [22]. The earliest use of the micro-CT was to study the bone structure and density [23].

2.1.2 Electromyography (EMG)

During the early 1960s, researches' focused on investigating EMG signals, by defining the muscle electrical signals, this diagnostic approach was used to evaluate muscles health and that of the controller nerve cells. It is known to mainly be used to study neuromuscular abnormalities, and its applications can be classified under two main categories 1) discrete movement recognition, and 2) Continuous movement recognition [24]. The Hills Models has been given as an example of continuous movement recognition in measuring muscle force and movement. It macroscopically reports the contraction of the skeletal muscle counteraction, where it helps to improve a number of contraction models for the calculations of muscles strength [25, 26]. In the cases where the neck has pinched a nerve, the EMG may help to determine if the effected nerves are working properly or not. EMG helps in the diagnostic of neck and shoulder pain.

2.1.3 Biomaterial used in Orthopedic Treatment

An extraordinary research attempt has been established via the development of biomaterials in sustaining of physiological activity and critical functions in the sustainment of life [27]. Bone plates have been used sufficiently in the repair of bone fractures. Conventionally speaking, biomaterials can be classified as the following types of materials; 1) metals, 2) polymers, 3) ceramics, 4) composites, 5) nano-composite, 6) natural biomaterials, and 7)nano-biomaterials. These materials can be used to repair any damages in the human body while simultaneously being compatible with the human biological system. As well as biocompatibility, these materials have suitable mechanical properties, vesicular stricter, high wear resistance, high corrosion resistance, Osseo integration, nontoxicity and longer fatigue life [28].Biomaterials have many application uses, such as in orthopedics, cardiovascular, tissue engineering scaffolds, ophthalmic, dental, wound healing as well as many other areas of use.

As well as, the mechanical properties of various metals and alloys have been extensively studied in the development of joint replacements. As in total joint arthroplasty, corrosion, toughness, stiffness, brittleness, ductility, and ease of machinability are all matters taken into account. The stress surrounding the implant is critical importance, which may be more substantial where the use of materials that differ significantly from the bone is seen. In addition, compatibility with computerized tomography (CT) and magnetic resonance imaging (MRI) are of particular concern in cervical disc arthroplasty for long-term evaluation of the implant and the surrounding structures, as it relates to any wearing characteristics and functional degeneration. To that end, four metals can be used in contemporary disc arthroplasty. For instance; Titanium, Titanium-based alloys, stainless steel alloys, and cobalt alloys. Table 1 shows the developed artificial cervical disc types which are approved by the FDA (US Food and Drug Administration).

Table 1: Artificial cervical disc device

Name	**Company**	**Consist of**		**Level**	**Range**
		Outer surface	**Inner surface**		
Mobi-C	Zimmer Biomet	CoCrMo	Polyethylene	Single level /2 level	C3 - C7
Prodisc-C	Depu-Synthes	CoCrMo	UHMWPE	Single level	C3 - C7
Bryan Disc	Medtronic	Ti	Polyurethane	Single level	C3 - C7
Secure-C	Globus	CoCrMo	UHMWPE	Single level	C3 - C7
Prestige LP	Medtronic	TiCeCs		Single level /2 level	C3 - C7
PCM	Nuvasive	CoCrMo	UHMWPE	Single level	C3 – C4 C6 – C7

2.2 Developments in Joint Modeling and Analysis

Based on the biomechanical response of the human body, and developed technology, it has become evident, that science can improve human health via the use of modern technology. These technologies are mainly composed of computers and computer software. To perform a correct analysis it is necessary to understand the human body, bone and joint structures.

Over the last four decades, the computational modeling of the biomechanical systems has been developed. An example of this is the publication of the earliest study on the viscoelastic conduct of biological tissue in 1968 [29]. This is known as the precursor of the Finite Element (FE) model. In 1971 FE was used in terms of development of a model of a femur, with the mechanical stresses investigations.

2.2.1 Development in Cervical Disc Modeling and Analysis

A kinematic model was developed to initiate rotation, flexion/extension, lateral flexion, and torsion. A study was published which focused on the effect of gravity and directional acceleration on action lines of muscles forces and external load; in order to obtain superior comprehension [30]. The results showed that joint reaction forces and muscle forces were not affected due to flexion. However, the forces between odontoid and ligaments transverse manifested the lowest level in flexion. Furthermore, a dynamic and deformable cervical FE model of C1 through to C7 with all disc levels and ligaments was used to quantify spine mechanics under complex loading conditions, in an effort to study injury risk under dynamic loading, thus a rigid body approach has been used and the disc and ligament properties were based on previous publication. The discs annulus showed a greater strain rate, it displayed posteriorly in the case of extension, but in the event of flexion it was, greater anteriorly. Additionally the load distribution between discs was influenced by anatomic variability [31].

In 2007, an FE 3D model was developed of C1 – C7, which was established based on CT data. The creation was made to study the effects of quasi static load on intervertebral discs, where it is assumed the discs are an incompressible object in to deformation, nonlinear and anisotropic. A solid volume definition was used to model the intervertable disc. The geometry was built based on the thickness of anterior and posterior mentioned in the literature review. The model took into consideration the unique structure of the human cervical spine [32]. A year later in 2008, validation has been received of the C4-C5 model, with a couple of in-vitro human cervical data, where it has been established and developed to prove accurate responses under different physiological loading levels to investigate ROM in flexion/extension [33]. Furthermore, validation of the FE model was observed via research developed to study the difference between the intact C5-C6 segment and artificial cervical disk (Bryan) at the same level. The results of the study pointed to optimized assist based on the quantification aspects for cervical disc replacement. It also shows that, the results of bending movements and compression in both cases were sufficiently meaning the Bryan disc is compatible with the physiological of the vertebral structure [34]. A study focused on finding three different scientific studies in order to decipher the best optimized artificial cervical disc device. Results showed the lumbers vertebral are actually subjected to lower bending load when compared to the cervical vertebra. TiCaP (titanium/calcium phosphate) (Cervitech, Inc., Rockaway, NJ) which is a coating of bony in growth can lead to 10% - 15% increased bony integration when compared to plasma-sprayed titanium. TiCaP creates a highly saturated solution of CaP at the point of the metal–bone interface, enabling re-precipitation of hydroxyapatite and superior bony integration. Knowledge of the sliding distance and the characteristics of wear in relation to conventional biomaterials (ultrahigh molecular weight of polyethylene, a cobalt and chrome) demonstrate that any generation of particulate debris should only be a very minor consideration with relation to cervical arthroplasty [35].

In further developments; [36] an FE model of C4–C6 was developed and validated against experimental data towards the end of the 19^{th} century. The model consists of both solid and shell elements. The higher posterior stress was at C4-C5, but the lower anterior column stress was at C4-C5. While the compressive stress in C5 was higher than stress in superior and inferior C4, C6 vertebral.

An investigation about the effects of two level arthroplasty and fusion on cervical spine kinematics has been studied in-vitro [37]. A Biomechanical analysis of the cervical spine after total disc arthroplasty was conducted with the application of an experimental and FE investigation, and the results showed that a disc replacement would be more advisable than a second fusion. Results also conveyed that motion was less in C4-C5 after the arthroplasty. Then again, studies, of FE model for C2-C7 was validated that focused on lateral bending, axial rotation, and flexion/extension, the mechanical and biomechanical behavior of the cervical spine. C4-C5 projected rotation at almost 2° in the case of bending, with 12MPa stress. C4-C5 and C5-C6 presented the most discrepancies between the analytical and predicted stress values [38].

With the use of the ANSYS software, a ball-on-socket artificial disc model was developed to study the wear in flexion/extension and rotation. UHMWPE (ultra-high molecular weight polyethylene) and titanium (Ti6A14V) were used to build up the ball-on-socket respectively. The results showed that the maximum flexion/extension was approximately 30% of the cycle, where it reached approximately 8°. On the other hand the maximum axial rotation angle was 4°, after 50% of the cycling load [39].

By contrast, Pro-engineer software was utilized to develop a model build up on CT data for the normal spinal cervical vertebra C0-T1, in order to study, axial rotation and coupled lateral bending. The study concluded that the maximum axial rotation was in C4-C5 5.3° ±1.5°. Additionally the coupled lateral bending C4-C5 was one of the levels that recorded the highest values 5.4° ±1.8°. In terms of extension couple with axial rotation, C4-C5 recorded 2.0° ±1.2°, despite its existence in the upper and middle level of the cervical vertebrae [40].

A study was conducted by [41] on three different developed models of artificial discs. By using ABAQUS software, this study has focused on the differences that can be observed among the artificial discs; 1) metal-on-PE, 2) metal-on-metal and 3) elastomeric core. In relation to the C4-C5 level, it can be observed that each of the artificial disc models was unique, due to its material definition, thus constraints were present with boundaries applied throughout each model. The models were based on hybrid loading protocols involving 1Nm of pure moment in case of flexion extension, axial rotation and lateral bending.

C4-C5 FE model was validated in further studies, under flexion/extension and tension, to study the impact scenarios. As a result it was accounted that kinematics and kinetic had no significant changes in case of flexion /extension, and vice-versa when it came to extension due to posture. In the case of ageing, the developed model did not show any significant changes, however this may be due to the same material properties being applied to each model and 90Nm/s was loaded to the model [42].

A modern FE model was created in 2016, in order to study the cervical vertebrae. Based on CT data and taking into consideration the bio-realistic geometry of cervical spine, ligaments and the geometry of IVD; the model showed that a normal disc area of C4-C5 level 21.8mm^2. Elastic isotropic were assigned to all parts of the mode, but each section defined its material properties separately [43].

2.3 Studies Focusing on Improving the Patient Conditions after Medical Treatments

Artificial cervical disc replacement is applied in the treatment of cervical disc narrowing. For such treatments, extensive follow-ups are necessary to ensure that the surgery was successful and efficient. The first design of elastic artificial cervical disc replacement was engineered by Fernstorm, by using spherical metallic balls. However, after the failure of Fassio'ssilastic disc, a number of patents were diagnosed for designs during the 1980s. These included mechanisms that would enable axial load dissipation using silicon cushions, fluid-filled inflatable bladders, bio-ceramic fabric, elastic polymer, springs or coils. Figure 5 shows the artificial disc after surgery [44].

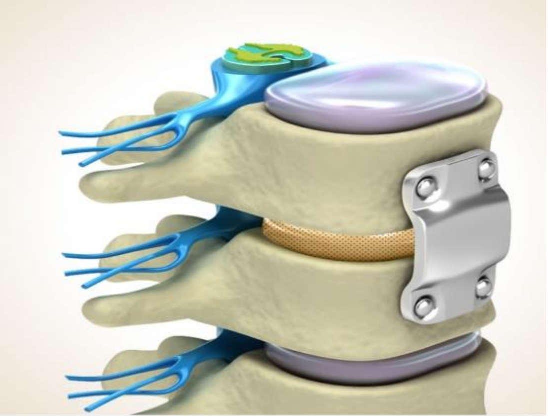

Figure 5: Artificial cervical Disc

2.3.1 Bryan Device and Patients Situation after Surgery

One of the recent artificial cervical discs is the Bryan disc, which is made of two metals; Ti as a shell and polyurethane as an inner mobile core. It was designed to be replaced by vertebrae discs from C3–C7.medical statistics based on data of 32 patients with artificial Bryan disc implant was studied and the data was collected continuously for four years, between the years 2006–2010, observing the severe cervical disc combination. Assessments were made by follow-ups with radiological flexion/extension. These assessments satisfied that there were remarkable and noticeable improvements, providing that, there has been no failure with any implant of Bryan device until now. [45] As an outcome of the above mentioned studies, the majority of the patients sustained good post-operative movability, with no sign of degeneration.

2.3.2 ADCF and Patient's Situation after Surgery

An example of a medical treatment and a solution for disc hernia is anterior cervical discectomy with fusion (ADCF). In this surgery the deteriorated part is removed, and replaced with ADCF disc, a gap may occur between vertebra and disc and this space can be filled by peek spacer that can fix it with a metal plate for stabilization; to avert slump in vertebral and scrap together.

ACDF patients have been advised to walk in order to clean the lungs, and pain must be controlled with analgesic beforehand. Patients can increase their activity by 10% after a short time. In addition, after two to three months, patients are required to attend physiotherapy sessions and can return to normal activities but are strictly prohibited from activities requiring high movements [46]. It is possible to feel weak after a surgical procedure that may disappear over time, but sometimes the feeling of numbness in the hand continues for a lifetime where this is rare [47].

2.3.3 TDR-C and Patient's Situation after Surgery

A backdated radiographic study was done to assess patients after cervical total disc replacement (TDR-C), a new approach of surgical treatment. This new surgical treatment conserves motion in the damaged part of cervical and out of the implementation of the artificial disc. Follow up results of TDR-C shows that ROM (range of motion) had extraordinary advancement (1.15 mm, $+5.67^{o}$). While the ACDF showed (0.12 mm, -0.96^{o}). Patients of ACDF recompensed for losing ROM. When using TDR-C, the total ROM in cervical significantly increase, maintaining the physiological distribution of ROM, which minimizes the probability of breakdown at the adjacent segment. [48].

Likewise, the Smith-Robinson technique has been used [49] to cover 95 cases, with a follow-up for 28 years with ACDF. A single level of ACDF was executed for 67 patients while the rest of the patients had two levels. Prior to surgery; 92 of the 95 patients complained that they were experiencing pain. Post-surgery only 24 patients still experienced some pain and in some cases, a second surgical procedure was necessary. During follow-ups, 14% was the neck disability indexes, with 5 scores meaning EQ-5D. Additionally good to excellent functional recovery was reported by 84.2%, while 96.8% were reported as satisfied. As a summary, pain release, high satisfaction, and increase in function were reported during follow-ups 25 years post-surgery, with 12% reported with adjacent segment disease (ASD).

2.3.4 Bristol Artificial Disc

The Bristol artificial disc was invented in 1998; however the development of the device began in 1989. A short follow up was recorded, showing that patients who complained from radiculopathy and utilized the Bristol device as treatment was noted as feeling better after surgery, and no degeneration nor any subsidence into the vertebra was reported, which in some cases may occur due to prosthesis. The design was developed until 2004 as Presting LP, [50] the follow up after Presting LP showed 0.2% temporary hemiparesis.

2.3.5 ProDisc-C Disc Prosthesis.

ProDisc-C received US FDA approval at the end of the year 2007. With the use of VAS and NDI, a shot follow-up study was conducted. The study showed post-operative improvements in functional consequence and also showed that ROM was improved. Similarly, no further pain was reported and there were no records of any complaints or device-related complications [50].

2.4 Contribution of the Current Research

Based on the literature review, there are only four types of material that can be used to design an artificial cervical disc, with specific material properties. In addition, the geometry of each artificial cervical disc was unique. Any artificial device must have the US FDA approval before it is available on the market. From the analysis point of view, the most accurate and applicable method of analyzing artificial cervical disc is via FEA. So far, some works have performed optimization by using the Taguchi method to establish the optimum design. Some were optimized via experimental in-vitro and in-vivo tests, by using human cadaver, and some others used an experimental approach and FEA at the same time. There are insufficient studies on the dynamic analysis. A few publications have focused on studying C4-C5 level exclusive.

There is a multitude of published papers relating to patient's situation and satisfaction after treatment, which also cover the side effects of surgeries and the difficulties.

In this study, the artificial cervical disc was designed with a different geometry which aimed to decrease the stress distribution to the vertebrae and the disc in order to improve the patient's daily activities, and decrease the problems caused by mechanical design.

Chapter 3

THEORY AND ANALYSIS

The objective of this study is to design an artificial cervical disc, for single level C4-C5, with the best applicable material CoCrMo with UHMWPE. Material properties and geometry were selected to be suitable in between the vertebral and compatible according to human anatomy, to obtain results close to natural anatomic disc. The FEA method is widely available, and has been used in many investigational analysis studies. Moreover, it is one of the more practical methods to achieve this objective in finding the artificial disc responses. This work aims to study the stress-strain distribution, which mainly focused on load response in cervical vertebra and artificial disc. To the purpose of study the ROM in: 1) axial rotation, 2) lateral bending and 3) flexion/extension, by applied moment in different directions. To add more value, dynamic analysis was also examined to study the model in case of injuries such as injuries related to car accident. Dynamic analysis can be done, by applying impact load or amplitude load to find the response of the same region. To achieve these objectives several steps were taken. The methodology of this works is presented in Figure 6.

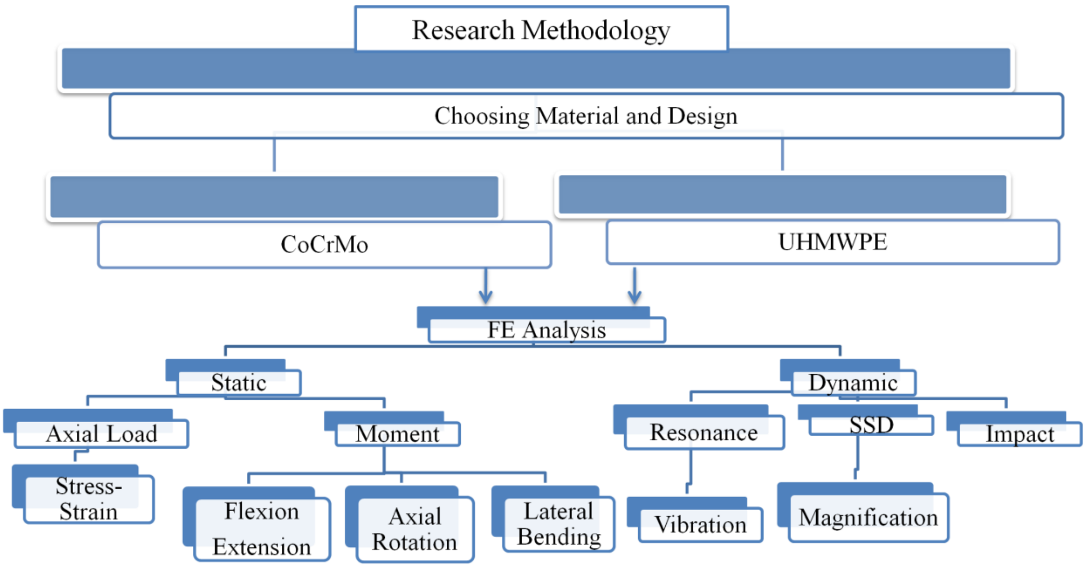

Figure 6: Research methodology

3.1 Cervical Vertebrae Modeling

Cervical vertebrae are very complicated and sensitive structures. Due to this issue, caution is required with creating and analyzing the model. The complexity of the structure makes it hard to design and analysis the vertebra.

For the purpose of analysis in the current study, the required cervical vertebrae were adopted from X-Ray of a volunteer with normal cervical vertebrae; the dimensions were recorded and drawn in ABAQUS (Dassault Systèmes Simulia Corp). The reason for building the geometry by ABAQUS is to avoid any contradiction in the geometry and meshing as would be the case if software was used to draw the geometry and then it had to be imported into ABAQUS. Figure 7 shows the C4 vertebral modeling.

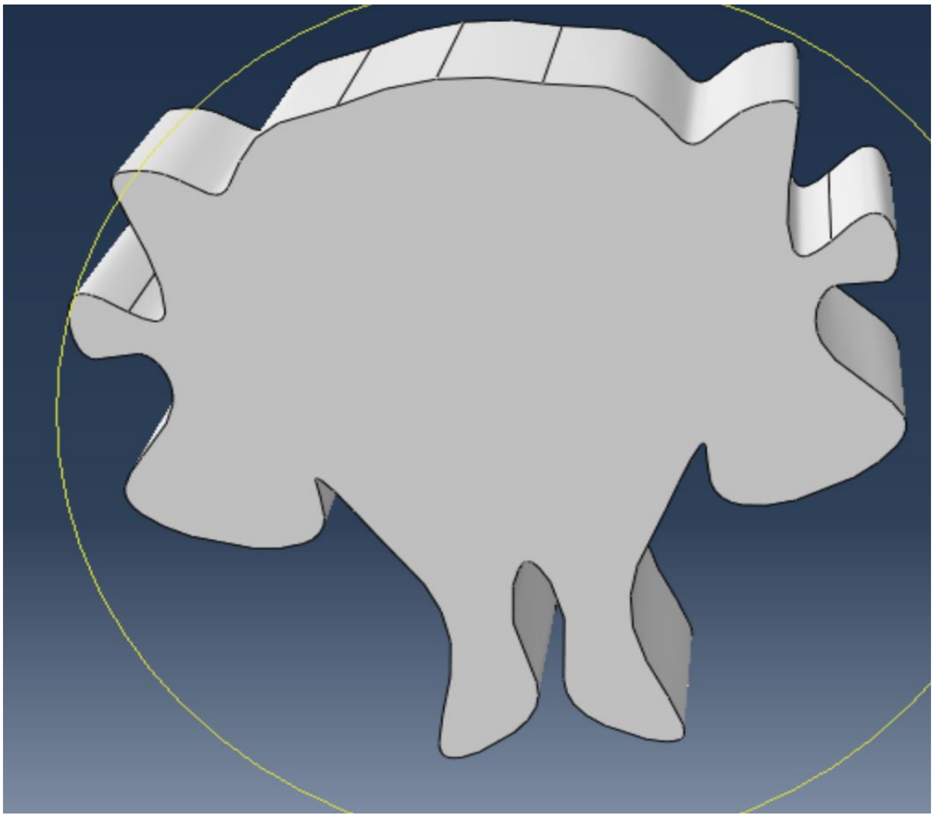

Figure 7: C4 Vertebral Model

3.1.1 Geometry of the Model

Conventionally, artificial discs are made up of two to three components, of metal and polymers. Metal and polymers both are advanced materials and preferable.

For the estimation of valid cervical vertebra design with the artificial cervical disc, and to avoid any complications in the design during the FEA, a single level of vertebral (C4- C5) were chosen to assemble and make the contact with the artificial disc as shown in the Figure 8 Vertebrae dimension were taken from published works [51]. Afterwards the ligaments were added, as shown in the Figure 9 if this process was not done as such, the resulting space between vertebral will cause complications during the analysis.

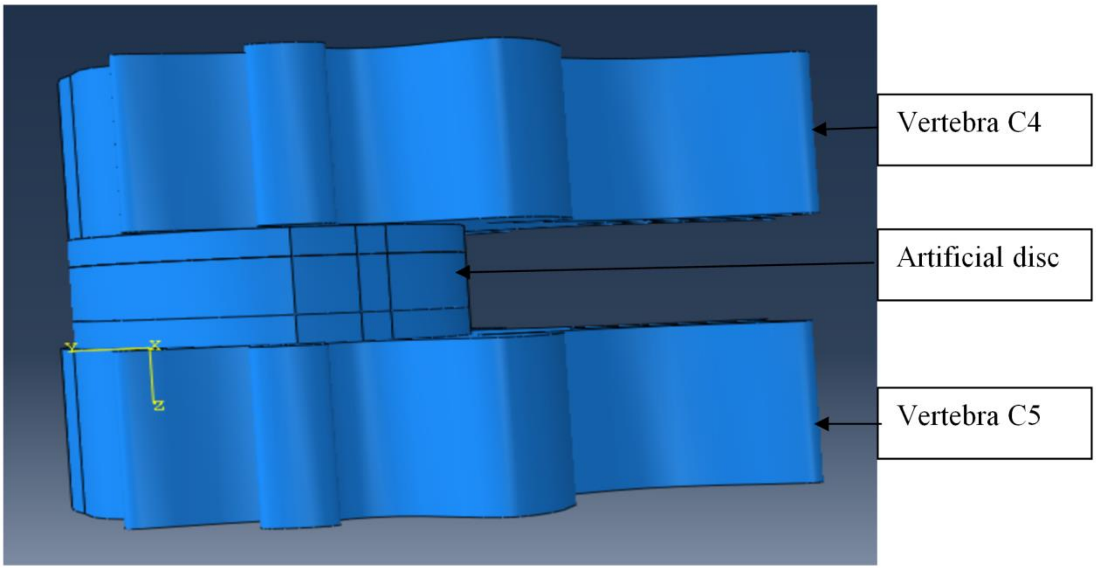

Figure 8: Single level of vertebra C4 – C5

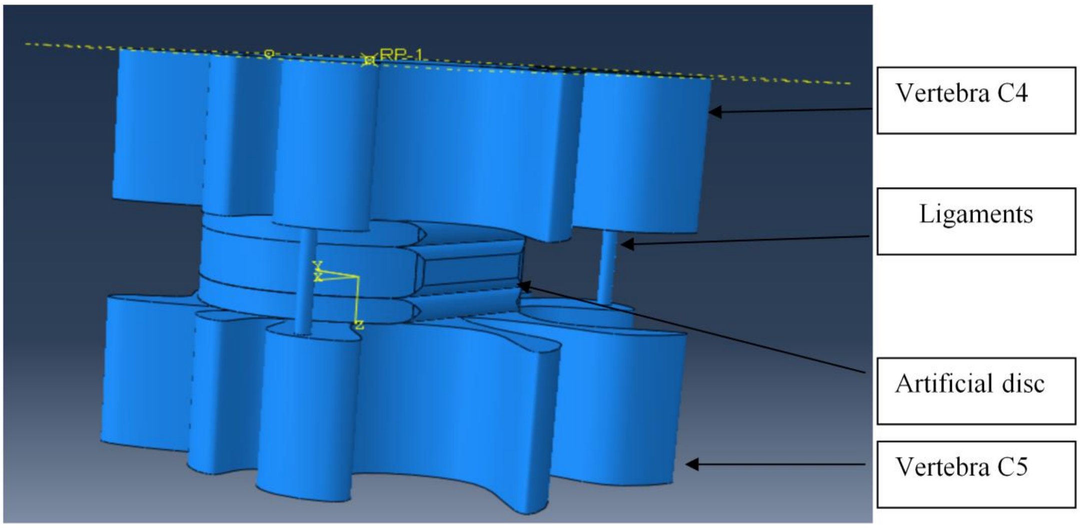

Figure 9: Vertebra Model with ligaments

Furthermore, the geometry of artificial disc is based on vertebral geometry and the anatomic cervical disc structure. By constructed it based on anatomic components, failure of the artificial disc according to design may be avoided. The design and dimensions of the artificial disc were constructed after studying the normal structure and previously developed artificial disc.

The total height of the artificial disc was 8mm with three layers. As upper and lower layers are 2mm for each and the middle layer is 4mm. The width 30mm, depth is 10mm. the design is shown in Figures 10 and 11.

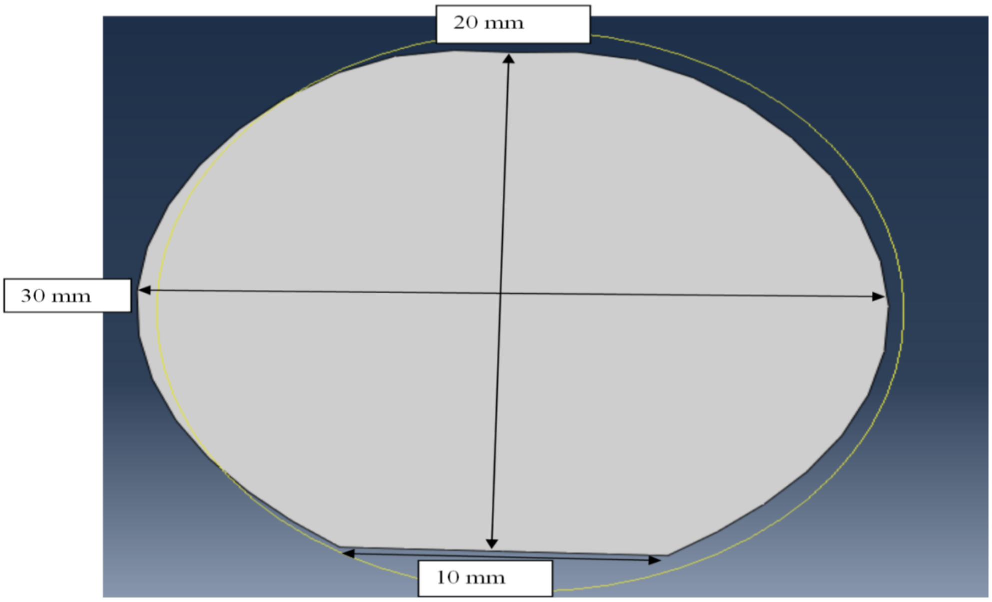

Figure 10: Top view of the designed artificial disc

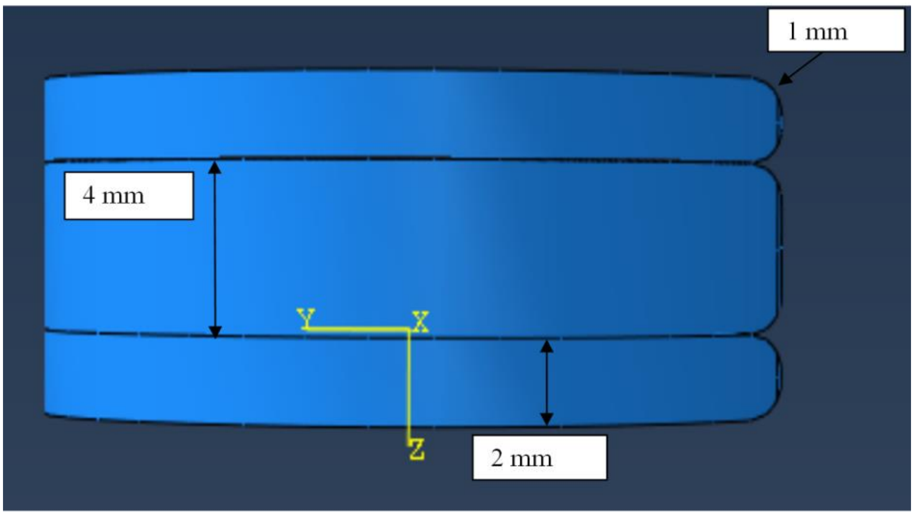

Figure 11: Side view artificial disc

The current disc design can be defined as a deformable core prosthesis design, which allows the motion of rotation to be free under load [52].

3.1.2 Material Properties and Modeling

The first step in FEA, after drawing the model is to define the material and material properties. Each part of the model is unique by itself, and it has its own properties and behavior. Table 2 shows the selected material for each part and their properties as it present that, C4-C5 cervical vertebra level, artificial disc structured is based on the approach of metal-on-PE; so CoCrMo and UHMWPE were chosen for this artificial disc. The material properties were chosen based on the literature review and published data [43, 53, 54, 57].

Table 2: Material properties of each part of C4-C5 vertebra level

Material	Density (Kg/m^3)	Young's Modulus (MPa)	Poisson ration	Properties	Reference study
(ITL) Ligaments	0.517	17.1	0.4	Elastic Isotropic Nonlinear	[43]
Vertebrae Bone	1900	20700	0.29	Elasticity Isotropic Nonlinear	[43]
UHMWPE	970	12000	0.46	Linear Elastic Isotropic	[53][57]
CoCrMo	8400	220000	0.29	Linear Elastic Isotropic	[54][57]

3.2 Continuum Mechanics

FE analysis cannot be accomplished without using continuum mechanics; because in finite elements, the mechanical behavior of the materials and the kinematics of the modeling, as discrete nodes and continuous mass are very important. In particular, this hypothesis is correct, since FEA deals with nonlinear problems. By using continuum mechanics, these types of problems can be solved through linearization. Linearization is where the problems are solved as linearly until it reaches the nonlinear problem. A good example of the use of this method in continuum mechanics is the Newton Raphson method.

The concepts of the finite element method are based on piecewise polynomial interpolation, where the piecewise technique is used in the entire model or structure in interpolated by connecting all elements together, and each node has its own set of simultaneous algebraic equations.

In general the solution to a nonlinear problem, solving for unknown **u** the final displacement (deformation) and **F** the applied force, the general Newton Raphson may be written as in the published book [56] and given by the Equation 3.1

$$DF(x_k)[u] = -F(x_k); x_{k+1} = x_k + u \quad (3.1)$$

3.3 Finite Element Analysis

In this section, the main steps followed in FEA are explained.

3.3.1 Defining C4-C5 Vertebra

Once the geometry was completed, the material definition was done under the same condition mentioned in Table 3.2.1. Density 1900 Kg/m^3, Young's Modulus 20700 MPa and Poisson ratio 0.29. In this study elastic isotropic material, was given as a definition of vertebra material

3.3.2 Defining Artificial Disc

By defining CoCrMo and UHMWPE both as elastic isotropic material; with the same condition of, density, Young's Modulus and Poisson ratio as given in Table 3.2.1

3.3.3 Defining Ligaments

Intratransverse Ligaments (ITL) were defined under the definition of elastic isotropic nonlinear material, with the same condition of, density, Young's Modulus and Poisson ratio as given in Table 3.2.1

Additionally, in all cases of defining material, the stress strain equations can be expressed in terms of material parameters where Young's Modulus E and Poisson ratio ν, λ and μ are the constant of material coefficients and J the volume ratio, as the Equation 3.2 [56].

$$\ln \lambda_\alpha = \frac{J}{E}\left[(1+\nu)\sigma_{\alpha\alpha} - \nu(\sigma_{11}+\sigma_{22}+\sigma_{33})\right]; \mathrm{E} = \frac{\mu(2\mu+3\lambda)}{\lambda+\mu}; \nu = \frac{\lambda}{2\lambda+2\mu} \qquad (3.2)$$

3.3.4 Create Boundary Condition and Load

The assembly was created and Tie constrains was chosen in order to connect each two parallel surface together (it gave the criteria of bonded for all parts, which means all the model will be under the same condition) as shown in Figure 12.

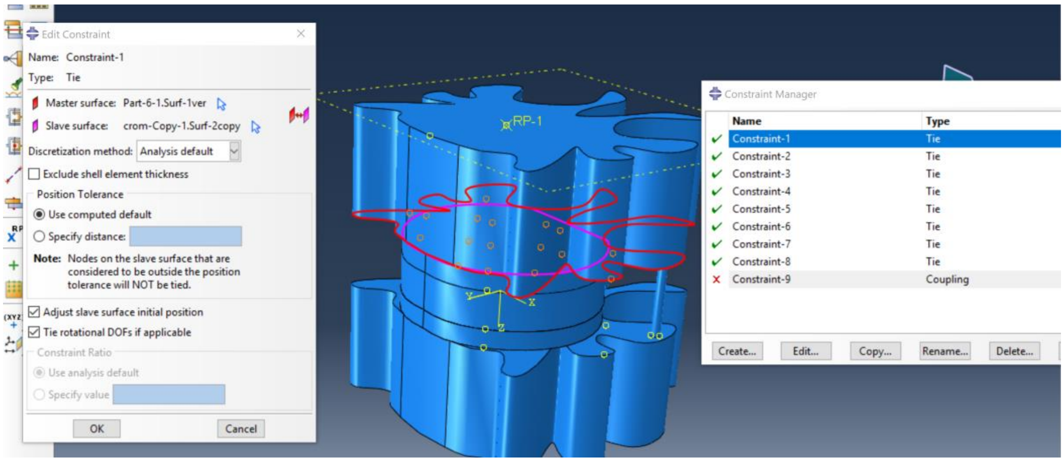

Figure 12: Tie constrains

In condition of applying axial pressure, fixed boundary condition was used as set Symmetry/Encastere to set all U1=U2=U3=UR1=UR2=UR3=0 end-plat of C5 assumed to be fixed as shown in Figure 13. Nevertheless, Pinned boundary condition (U1=U2=U3=0) were used when applied moment and shown in Figure 14.

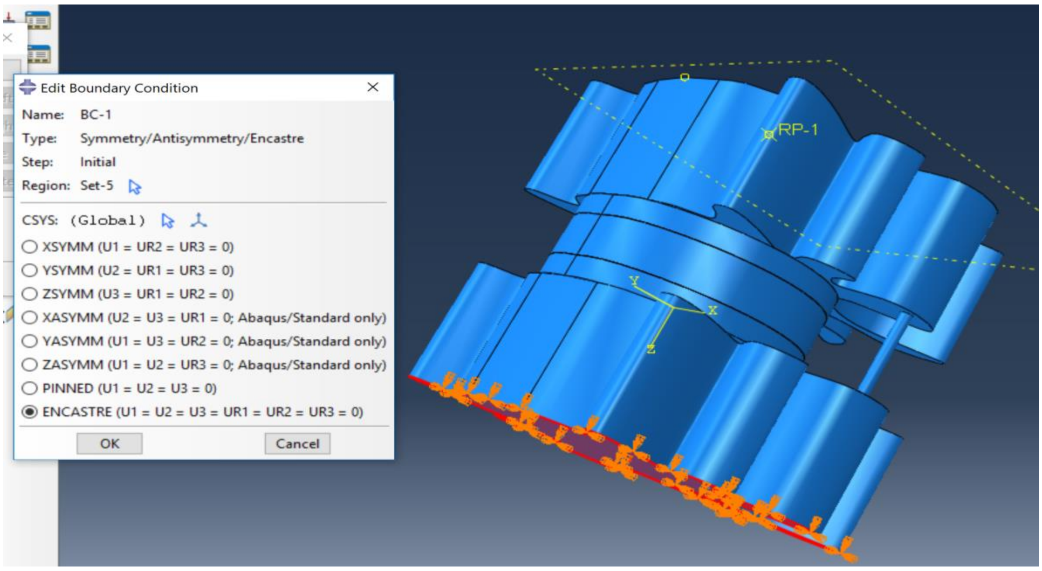

Figure 13: Fixed boundary condition at C5

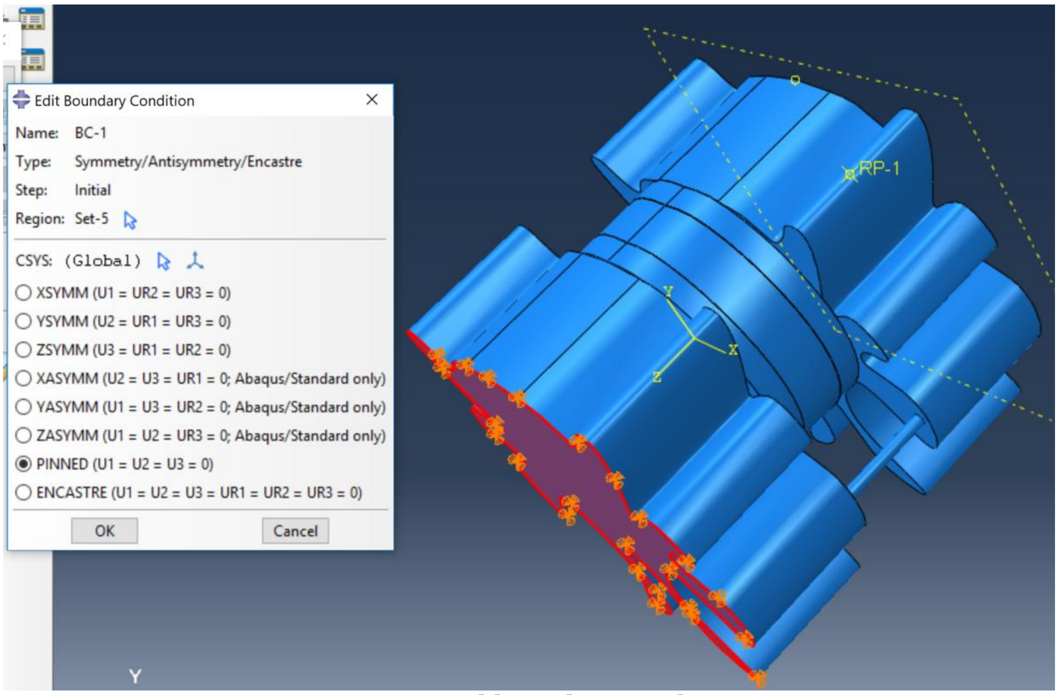

Figure 14: Pinned boundary condition at C5

The basic Equation of boundary conditions is 3.3 [56] Additionally, the simultaneous algebraic equations in the FEM is 3.4 where K is the property in the case of this study the elastic material had a stiffness property, u as the displacement behavior, and F for the action of force. The unknown is the displacement behavior, so the Equation 3.4 [57] is changed to the Equation in 3.5 [56].

$$\text{Boundary conditions: } B(\varnothing) + g = 0 \tag{3.3}$$

$$\text{Simulation algebraic: } [K][u\} = \{F\} \tag{3.4}$$

$$u = [K]^{(-1)}\{F\} \tag{3.5}$$

In order to study stress strain failure and force-displacement, static axial pressure was applied as shown in Figure 15. None the less, the second load case was investigated and fined the amount of lateral bending, flexion/extension, and axial rotation to compare and validate the results with the literature review under quasi static condition.

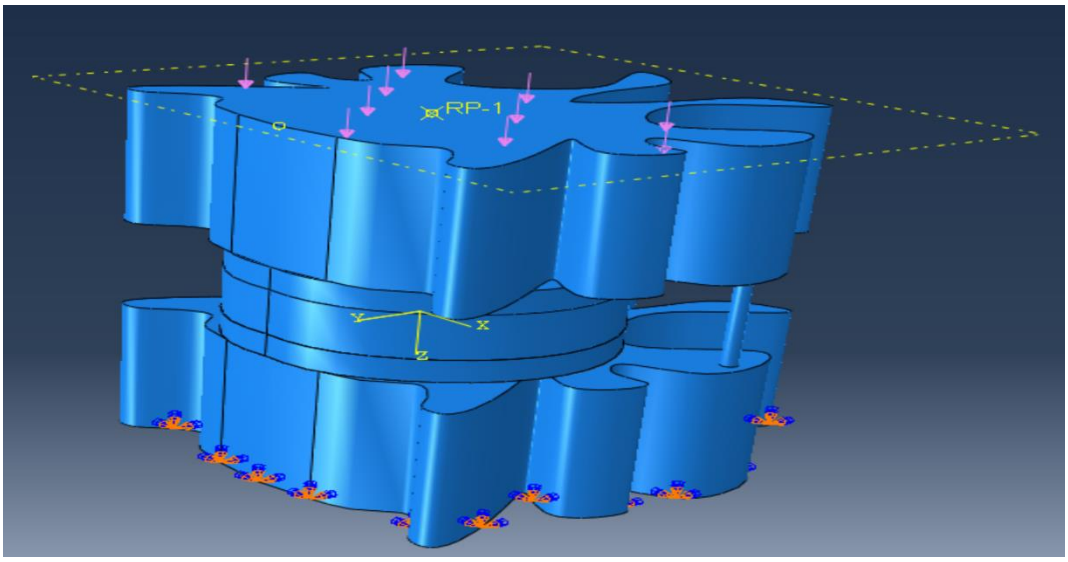

Figure 15: Axial pressure

Whilst, frequency step was created to find the normal mode of vibration, before applying the dynamic load, which leads to understand the effect of dynamic load on the model; it also helps to understand the normal motion of the model.

3.3.5 Creating the Mesh

Following this steps, the last step in creating the FE model is choosing the type of elements and meshing each part separately, in this model brick element where chosen to create the mesh which consist of 8 nodes method (Hexagonal element). Table 3 clearly shows the element type and the number of elements for each part.

Table 3: Element types of meshing FE model

Model Part	Element Type	Number of elements
C4	C3D8R	1532
C5	C3D8R	1532
ITL (ligaments)	SC8R	3944
CoCrMo (outer layers)	C3D10	346× 2 for two plates
UHMWPE (inner layer)	C3D10	295

Where:

C3D8R Linear brick element, with reduced integration point

SC8R Continuum shell element enhanced hourglass control formulation

C3D10 General tetrahedral element 4 integration points

It can be seen from the data in Table 4 the information's of model size, this model was prepared to study deformation, stress-strain and range of motion, in different cases such as axial rotation, lateral bending and, flexion-extension and the effect of dynamic load.

Table 4: Model size

Variable	Total Number
Total elements	26482
Nodes	39423
Nodes define by the user	39423
Total variables	119940

3.3.6 FEA Model Analysis

For the purpose of stress strain analysis, and to examine the deformation in the artificial disc the static load was applied, and the relation between stress strain, force displacement and compression are presented in chapter 4 and explained clearly. What's more, to analyze the ROM with artificial disc; moment was applied in different direction X, Y, Z and findings are presented with comparison to published data.

Moreover, in order to understand the effect of dynamic load, the frequency analysis has been done firstly; to find the normal mode of vibration. Secondly the dynamic analysis was processed under different load condition such as; stead state dynamic and tabular load, results are shown in chapter 4.

Chapter 4

RESULTS AND DISCUSSION

The geometry was modeled using 26482 elements, connecting 39423 nodes. Each node has the following displacement vectors Equation (4.1). This model is constructed on the base of brick element for vertebral and ligaments, which means it is independence on rotation. Though, tetrahedral element is used for the artificial disc.

$$U = \{U_1 U_2 U_3\}^T \qquad (4.1)$$

The structure is considered in FEA as brick and tetrahedral elements, which produces the following boundary condition Equation (4.2).

$$U_{x=0} = 0 \qquad (4.2)$$

4.1 Static Analysis

4.1.1 Axial Load (Pressure)

To study the axial motion, and the effects of axial load on the model, axil pressure is applied on the upper surface of C4, with fixed boundary condition on the bottom of C5 as shown before in Section 3.3. Figure 16 shows an overview of the maximum and the minimum misses stresses. Were it is noticeable that the largest amount of deformation occurs on the upper layer of artificial disc CoCrMo.

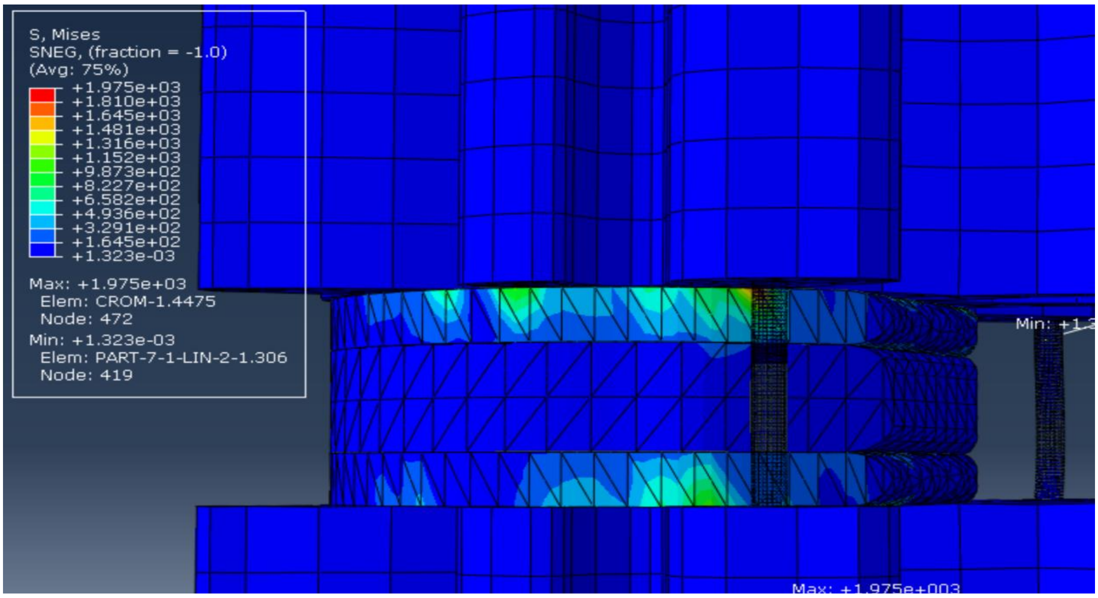

Figure 16: Maximum deformation

To have more valuable and accurate results a set of nodes (82-87) as shown in Figure 17 were selected to find the maximum stress in the outer layer of CoCrMo. And the numbers associated with the change of color gradients are an indication of the amount of stress the model is exposed to. As the color gradient changes from blue to red, the risk increases. And from this change we observed the highest stress at node 82 with 1.975e3 MPa. Furthermore the stress-strain curve was evaluated for each node separately as shown in Figure 18 and compared. This comparison confirmed that the value of the maximum stress is at node 82, and likewise indicates that the yield strength (140$\pm$ 5) MPa, and the failure occurs at 0.004%. Notably, the plastic region starts at 0.000657 approximately.

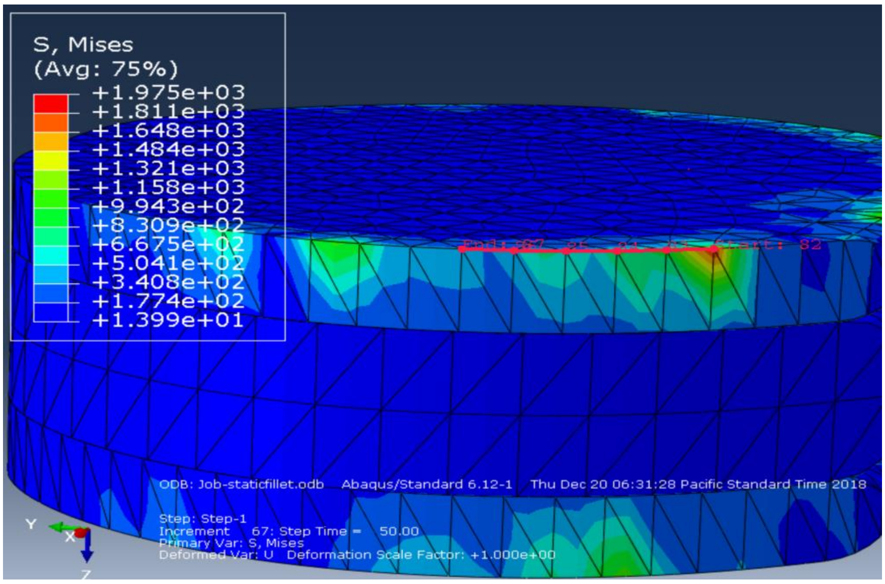

Figure 17: Set of nodes (82-87)

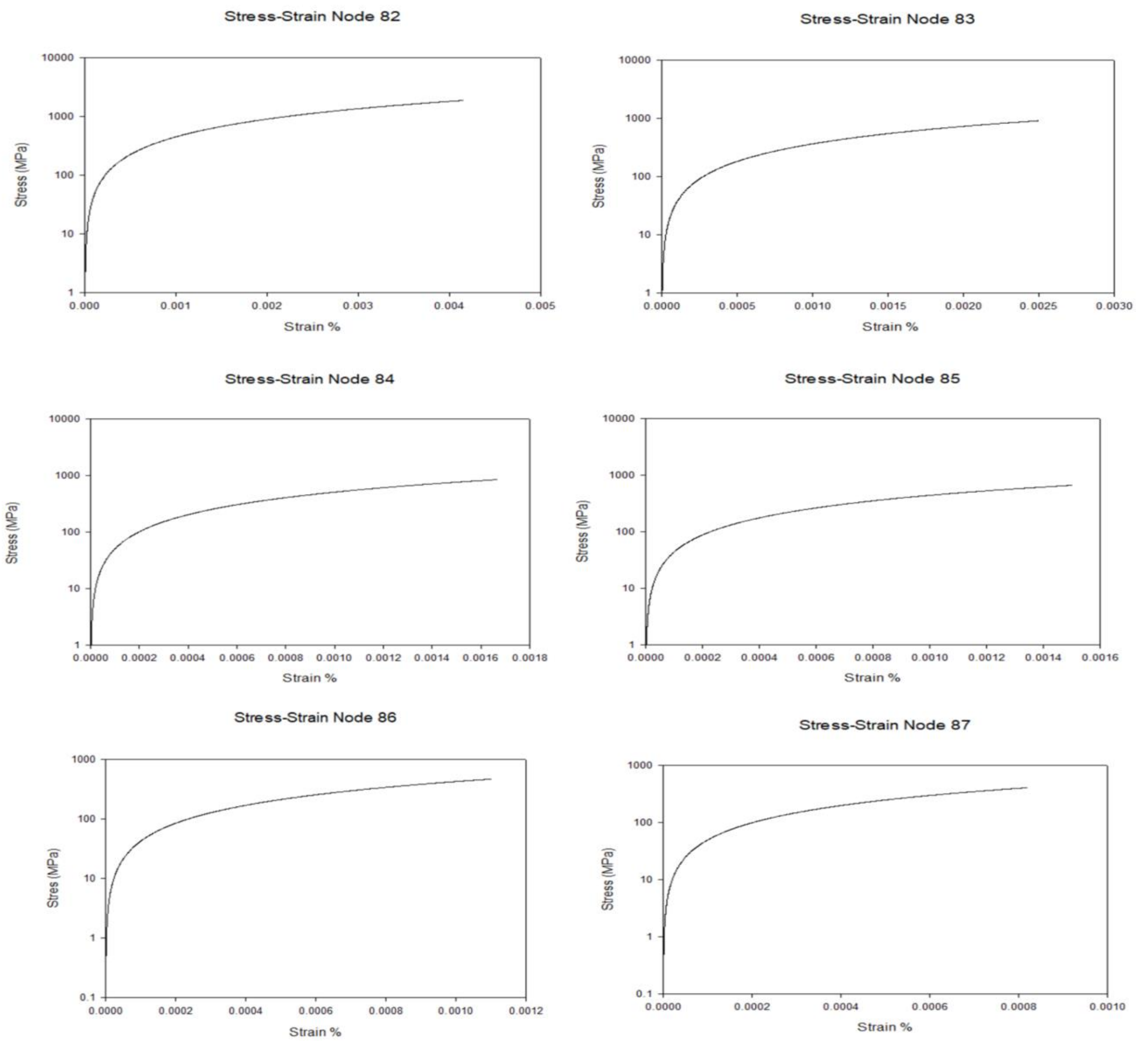

Figure 18: Stress-strain curves for selected nodes

Another important finding is force-displacement evaluation under different quantity of pure compression load, the relation between force and displacement in all direction, was investigated as provide in Figure 19 the results obtained from the preliminary analysis shows clearly the highest linear distribution in displacement was in U3 axes, and this is expected due to; the load direction applied in U3, and this result significantly agree with published data.

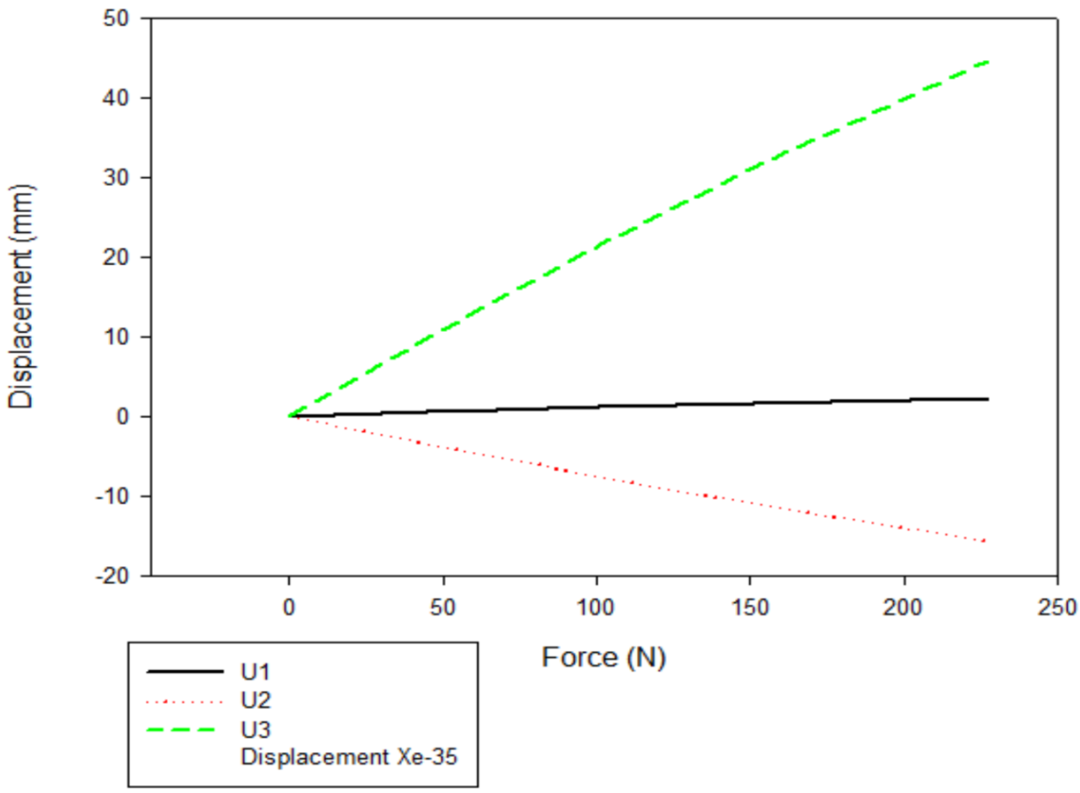

Figure 19: Fore-displacement distribution

The model behavior under compression was examined to find the highest response part as shown in Figure 20. Negative value provides that, the model is subjected to compression. The artificial disc which consist of two outer layer of CoCrMo and inner layer of UHMWPE results shows that, in case of having degeneration there will be no decreasing of the artificial disc highest; which means in biomechanics point of view, it can work in the exact approach as a transmission between vertebral to translate the external in the physiological environment. Very often it is important to find the compression on the annual fiber of the natural disc; similarly compression on the artificial disc. The maximum amount of compression may occur at the ligament. This result significantly follows the same sequence of [50].

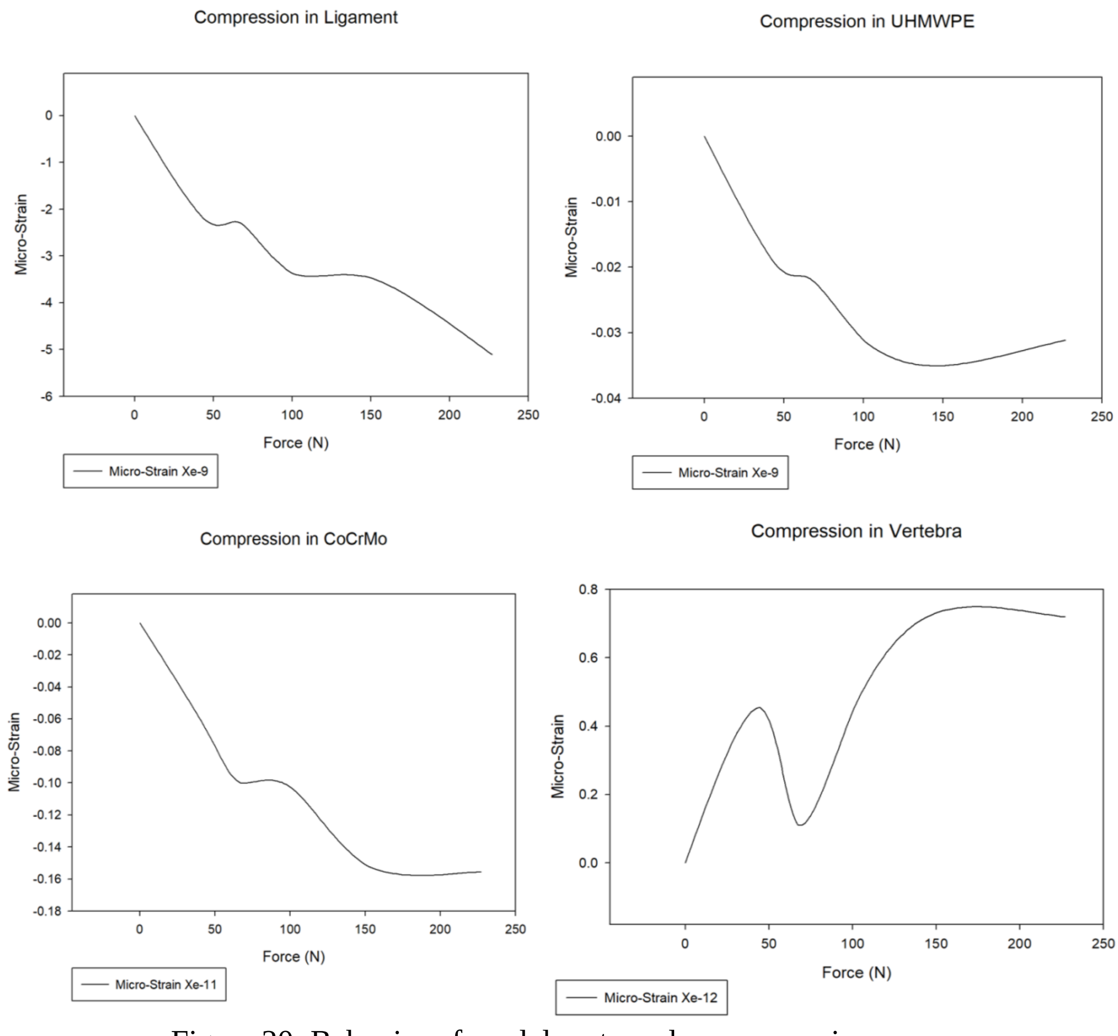

Figure 20: Behavior of model parts under compression

4.1.2 Range of Motion (Moment Load)

The model was examined under moment in three different directions X,Y,Z. as explained before in Chapter 3, in order to evaluate ROM in; 1) axial rotation, 2) lateral bending, 3) flexion/extension. Where the load applied in Nmm with case load varied from 0 to 2500 Nmm. Furthermore the ROM was defined as an angel. Figure 21 compare the results obtained from the FEA with previous published data to enhance data validation.

To give an illustration, the bar chart shows that in case of flexion/extension the presented FE model allow for a largest range of motion than experimental data [33,56] for instance, FE model records 5.36^o and 5.89^o in flexion/extension respectively, while in [33]5.1^o in flexion 5.0^o extension, and [56] 5.17^o flexion 4.51^oextension. However, the presented model record less ROM in lateral bending with 7^o. While a similar ROM for axial rotation comparing to published data.

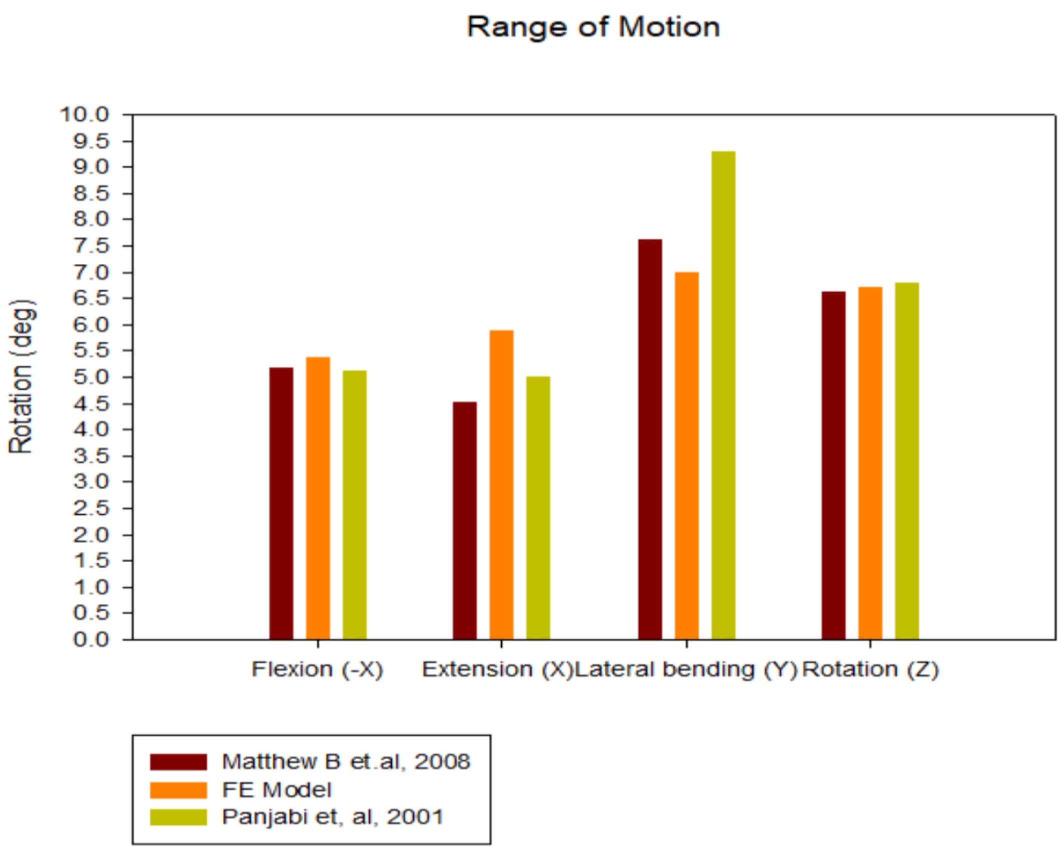

Figure 21: Range of motion

To add more value for this work, the flexion/extension results has been compared with published results for FE analysis [32,57,58] for both cases normal disc and artificial disc (Bryan)[58], as shown in Figure 22 where minus sign indicates the flexion ROM. The most interesting finding was that present FE modal and Bryan artificial disc has almost the same range of flexion/extension ROM. In general, the behaviors of this result indicate that, this work results quite similar to the previous treatises results.

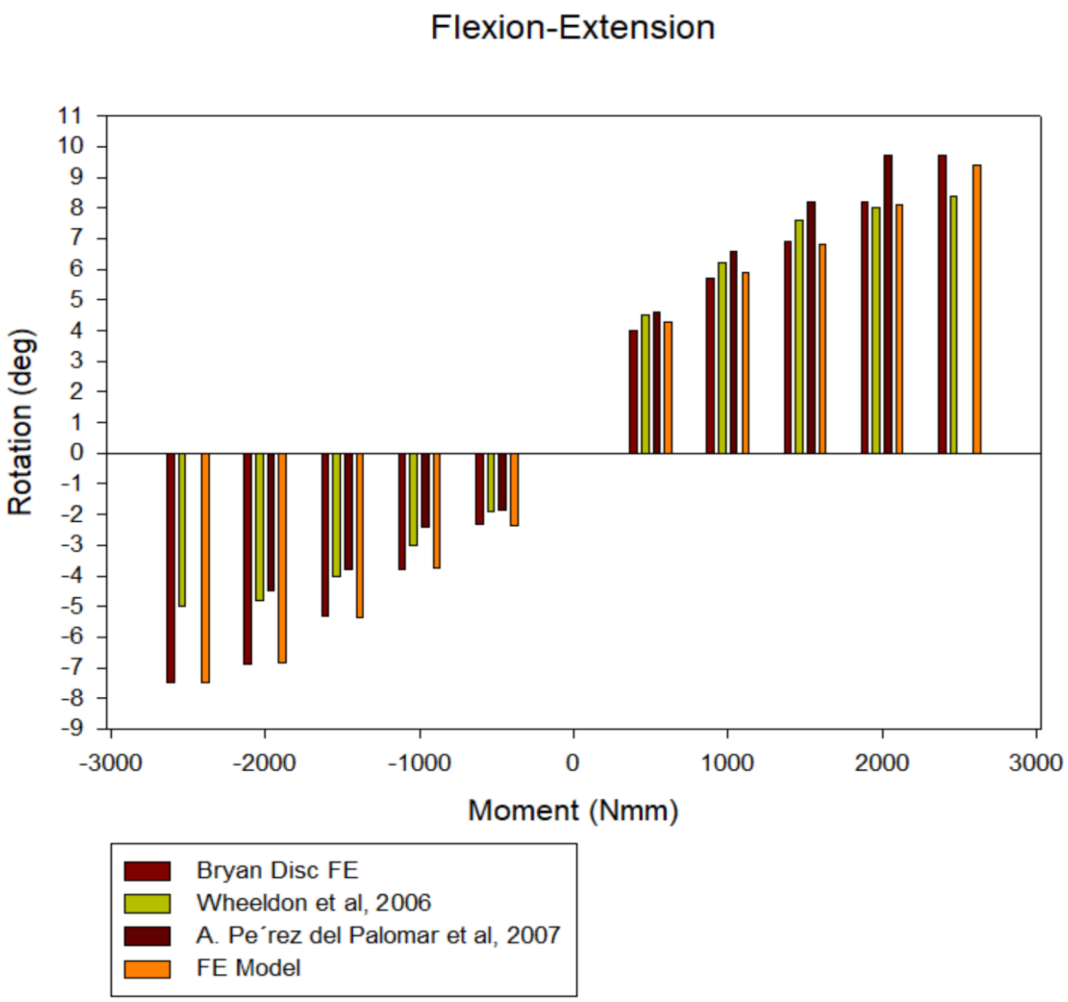

Figure 22: Flexion/Extension

4.2 Normal Mode of Vibration

Since it is necessary to introduce the dynamics referring to the basic free motion analysis, it is vital to extract the normal modes of vibrations for such complex structure. The FE model described above was solved for eigenvalue problem producing the results presented in Table 5. Where U1 U2 U3 are the displacements vectors in X, Y, and Z axis respectively. The most critical modes are represented in Figure 23.

Table 5: Natural frequencies of the structure

Mode No.	Freq. (Rad/s)	Freq. (Hz)	Dominant motion
1	1126.6	179.30	U2
2	1253.8	199.55	U1
3	1606.4	255.67	U1
4	2001.1	318.48	U1
5	2010.9	320.05	U2
6	2011.7	320.18	U1
7	2209.2	351.61	U1
8	3003.1	477.97	U3U2
9	3304.3	525.90	U1
10	3620.0	576.14	U3
11	3661.3	582.71	U2U3
12	3661.3	582.71	U1U3
13	3661.5	582.75	U2U3
14	3661.5	582.75	U1
15	3661.5	582.75	U1U3

As indicated in the table and the model shape Figure 23. The model was influence by the first mode, where a fundamental normal mode is the lateral normal bending mode with frequency 179.30 Hz in Y direction. The forth mode in X direction is bending at 318.48 Hz while eightieth frequency 477.97 Hz is a second lateral normal bending. The 9th mode shows like a twisting mode is started with 525.90 Hz. In light of, the critical modes, in which the artificial disc can be affected, are the 4th mode and mode 13th.

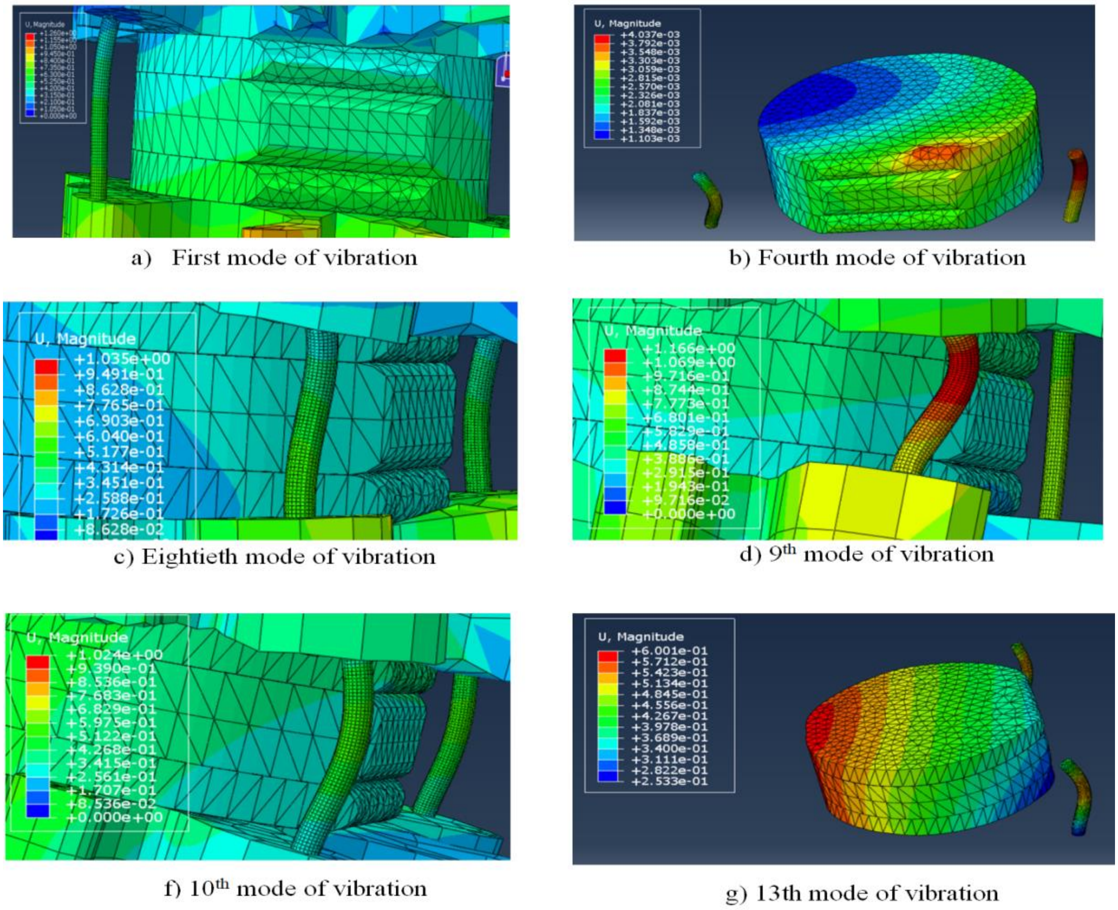

a) First mode of vibration
b) Fourth mode of vibration
c) Eightieth mode of vibration
d) 9th mode of vibration
f) 10th mode of vibration
g) 13th mode of vibration

Figure 23: Normal response

4.3 Dynamic Analysis

Based on normal response results, a steady-state dynamic step was created to study the relationship between displacement and frequency. An assumption of structural damping with 5% constant has been assumed with applying concentrated force on the artificial disc. There was no damage on the artificial disc the deflection occurred on ligaments only as clarified in Figure 24 which means the artificial disc is strong enough and can care this situation of load without injury damages.

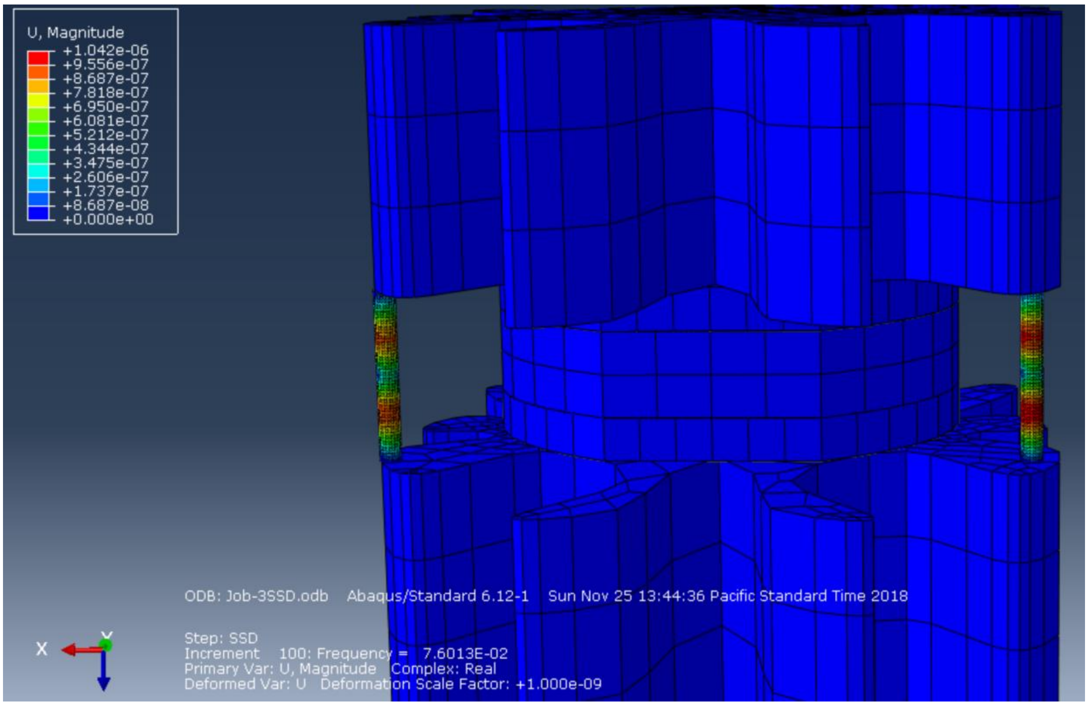

Figure 24: The effect of steady-state dynamic

A decision of select 1 node on ligaments has been take to evaluate how dose lower and high frequencies may effect on displacement in the three spatial directions (U1U2U3). The dynamic response of the selected node 1158 is shown in Figure 25 the highest displacement distribution is in U2 in between 0.01 Hz and 0.1 Hz. On the other hand the lowest distribution in U3. While U2 record the maximum frequency 250 Hz with zero displacement.

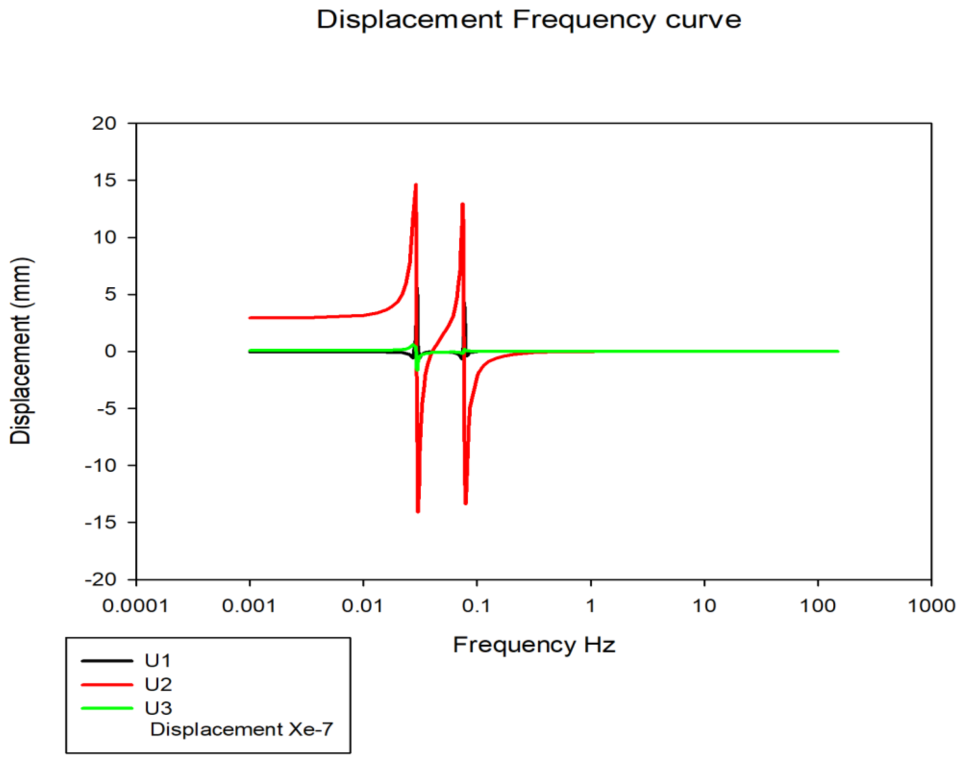

Figure 25: Dynamic response of the selected node

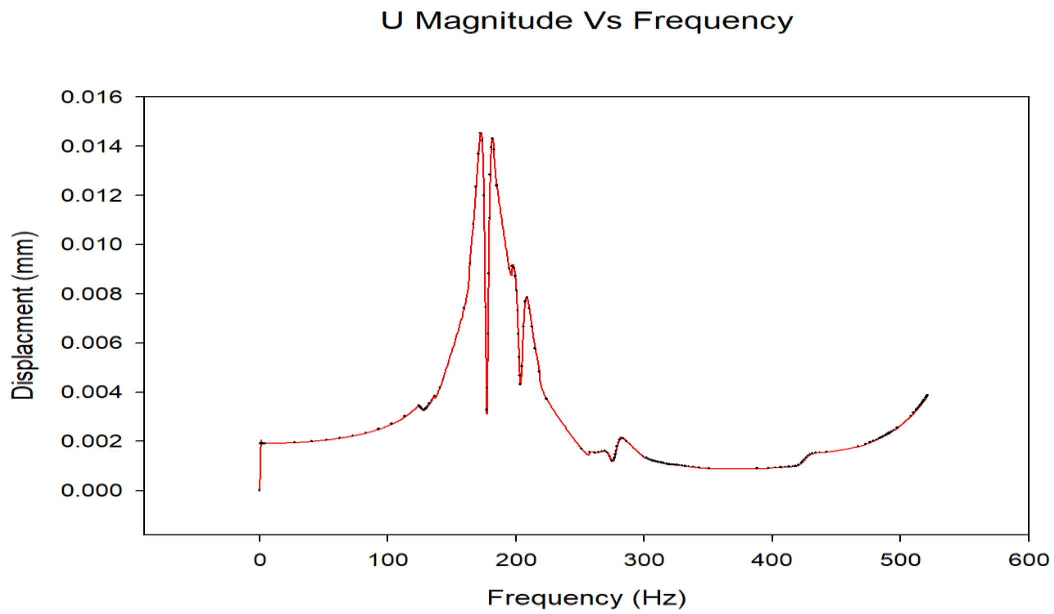

Figure 26: Displacement magnitude under frequency

The present study was designed to determine the effect of dynamic load on artificial disc Due to the importance the correlation between displacement and frequency; Figure 26 shows displacements as a function of normalized frequency (driving frequency/ natural frequency of main mass). Moreover, provides the relation where, the magnification occurs around 0.015 when applying 100N which cause a lateral bending with 180 Hz causing the resonance condition. However a torsion resonance is shown at 280Hz. Where anti resonance occurs at 0.0025. Moreover, a second lateral bending with small quantity occurs at 450Hz attention toward zero by $^{w}/_{w_n}$ displacement is around 0.0019. While during the resonance count it reaches 0.015, which means eight times higher.

As a conclusion of this type of analysis and load, the lower natural frequency are very dangerous, where the load will give a mode shape cross-bonding to a lower natural frequency; which lead to have a very high magnification factor.

By applying a cycling tabular loads with amplitude, which enhance finding the amount of stress in case of having deformation in artificial disc by injuries and accident. As presented in Figure 27. The maximum amount of strees at the lawer layer of CoCrMo. However, it should be noted that the cause of this stress on the edges is the sharp edges of the design, which should be avoided in the design in general and in the FE analysis.

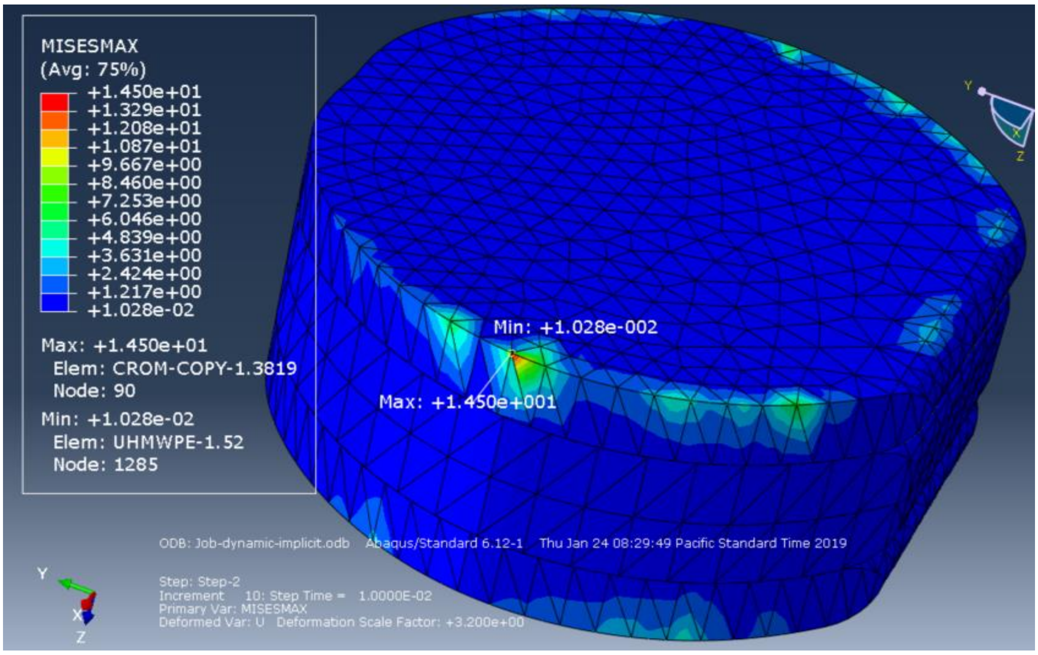

Figure 27: Stress distribution along true distance direction

Chapter 5

CONCLUSION

The purpose of the current study was to design artificial cervical disc at the C4-C5 level, and to investigate this disc design under; 1) axial load, 2) moment load, and 3) dynamic load. In view of analyze stress-strain distribution, ROM in (axial rotation, lateral bending, and flexion/extension), and the normal mode of vibration and impact of accident/collisions in artificial disc. The FE model was examined using the principle of material, geometric nonlinearities and brick element (hexahedral mesh 8 node methods) for vertebra and ligament, and tetrahedral element was used for artificial disc.

Based on the results of axial load, this research extends our knowledge of the linear relation between applied force and displacement, and the linear relation of stress-strain. Furthermore, the maximum deformation occurs in artificial disc in CoCrMo layer which means the artificial disc works as a damper that absorbed the load. As well as, the compression load record the maximum micro-strain in ligaments, the results significantly follows the same sequence comparing with published data.

Importantly, the current investigation was limited to the analysis of the artificial disc. Accordingly, vertebral modeling was not treated accurately with the exact anatomical model, to that end; results may have differences, with published data of anatomic model. Notwithstanding these limitations, the study present valid and similar data compared to published data of Bryan artificial disc, in ROM of flexion/extension and this is one of most obvious finding to emerge from this work. Although, in the current model CoCrMo and UHMWPE is used for the structure of outer and inner surface respectively, while Bryan disc consist of Ti and Polyurethane respectively.

In view of ROM in axial rotation and lateral bending findings, current results were compared and validated against several published data of experimental and FE of anatomic disc. However, the validation of this analysis is limited due to the lack of researches of analyzing implanted artificial disc at C4-C5 after surgical replacement.

The second major finding was normal response which presents the normal mode of vibration and observes the most dangerous frequency range that may affect the artificial design and ligament. With this in mind, the steady state results provide information about the maximum deflection, the artificial disc did not effect and the maximum deformation was on ligaments. Nonetheless, a tabular load with amplitude shows the maximum amount of stress in case of having deformation in the artificial disc.

The evidence from this study suggests that using elastic material definition to define ligament, will give more accurate results of analyzing the ligaments by using FE method. The study has confirmed the findings of [56], which found that artificial disc, can offer a similar ROM of anatomic disc for patients. Not to mention that, this is the first study reporting dynamic analysis for artificial cervical disc design between C4-C5 level exclusive.

One source of weakness in this work; the linkage of anatomic source for vertebrae and ligaments, to enhance the analysis result, it is required to take this point into consideration in future work. Considerably more work will need to be done to determine the effect of changing the geometry.

Finally it would be interesting and more valuable, to do experimental test and FE method and compare between both methods.

REFERENCES

[1] Neumann, D. A. (2017). Kinesiology of the musculoskeletal system: Foundations for rehabilitation 3rd ed. *St. Louis, MO: Mosby Elsevier*, *350*, 368.

[2] Cervical Activities Booklet: The Six Movements of the Neck. (2019). Retrieved from https://www.brain-spine.com/cervical_activities/six_movements_of_the_neck.html

[3] Bogduk, N. (2005). *Clinical anatomy of the lumbar spine and sacrum*. Elsevier Health Sciences.

[4] Humzah, M. D., & Soames, R. W. (1988). Human intervertebral disc: structure and function. *The Anatomical Record*, *220*(4), 337-356.

[5] Mattucci, S. F., Moulton, J. A., Chandrashekar, N., & Cronin, D. S. (2012). Strain rate dependent properties of younger human cervical spine ligaments. *Journal of the mechanical behavior of biomedical materials*, *10*, 216-226.

[6] Niagara Spine Clinic. Treating Cervical Disc Herniations. (2019). Retrieved from https://www.graychiropractic.ca/portfolio-item/cervical-disc-herniation/ . Lali Sekhon, F. (2019).

[7] Ramana, K. V. (2015). A Fully Automated New-Fangled VESTAL to Label Cervical Vertebrae and Intervertebral Discs. *Procedia Computer Science*, *57*, 483-492.

[8] Li, Z., Wang, H., Li, L., Tang, J., Ren, D., & Hou, S. (2017). A new zero-profile, stand-alone Fidji cervical cage for the treatment of the single and multilevel cervical degenerative disc disease. *Journal of Clinical Neuroscience, 41*, 115-122.

[9] Liu, F., Komistek, R., Mahfouz, M., & Cheng, J. (2006). In vivo determination of the dynamics of normal, fused and disc replacement cervical spines. *Journal of Biomechanics*, *39*, S133.

[10] Zhang, Q. H., Teo, E. C., Ng, H. W., & Lee, V. S. (2006). Finite element analysis of moment-rotation relationships for human cervical spine. *Journal of biomechanics*, *39*(1), 189-193.

[11] Prasher, A., & Tay, B. (2015). Treatment of Spinal Conditions in the Young Adult: Endoscopic Cervical Foraminotomy. *Operative Techniques in Orthopaedics*, *25*(3), 217-224.

[12] Jho, H. D. (1996). Microsurgical anterior cervical foraminotomy for radiculopathy: a new approach to cervical disc herniation. *Journal of neurosurgery*, *84*(2), 155-160.

[13] Cervical disc degeneration[Video]. (2009, May 22). FutureHealthInc. Cervical Vertebra. (n.d.). Retrieved September 20, 2018, from https://prohealthsys.com/central/anatomy/grays-anatomy/index-10/index-10-2-2/cervical_vertebra/

[14] Markatos, K., Tsoucalas, G., & Sgantzos, M. (2016). HALLMARKS IN THE HISTORY OF ORTHOPAEDIC IMPLANTS FOR TRAUMA AND JOINT REPLACEMENT. *AMHA-Acta medico-historica Adriatica*, *14*(1), 161-176.

[15] Charnley, J. (1972). The long-term results of low-friction arthroplasty of the hip performed as a primary intervention. *The Journal of bone and joint surgery. British volume*, *54*(1), 61-76.

[16] Smith, L. (1963). Ceramic-plastic material as a bone substitute. *Archives of Surgery*, *87*(4), 653-661.

[17] Ranawat, C. S., & Sculco, T. P. (1985). History of the development of total knee prosthesis at the Hospital for Special Surgery. In *Total-Condylar Knee Arthroplasty* (pp. 3-6). Springer, New York, NY.

[18] Sun, S. N. M., Gillott, E., Bhamra, J., & Briggs, T. (2013). Implant use for primary hip and knee arthroplasty: are we getting it right first time?. *The Journal of arthroplasty*, *28*(6), 908-912.

[19] Zhu, Z., & Shen, Q. (2008). The Research of Artificial Cervical Disc Replacement. *Journal of Nanjing Medical University*, *22*(6), 335-337.

[20] Lewis, G. (2001). Properties of crosslinked ultra-high-molecular-weight polyethylene. *Biomaterials*, *22*(4), 371-401.

[21] Link, H. D., McAfee, P. C., & Pimenta, L. (2004). Choosing a cervical disc replacement. *The Spine Journal*, *4*(6), S294-S302.

[22] Clark, D. P., & Badea, C. T. (2014). Micro-CT of rodents: state-of-the-art and future perspectives. *Physica medica*, *30*(6), 619-634.

[23] Rüegsegger, P., Koller, B., & Müller, R. (1996). A microtomographic system for the nondestructive evaluation of bone architecture. *Calcified tissue international*, *58*(1), 24-29.

[24] Latwesen, A., & Patterson, P. E. (1994). Identification of lower arm motions using the EMG signals of shoulder muscles. *Medical engineering & physics*, *16*(2), 113-121.

[25] Naeem, U. J., Abdullah, A. A., & Xiong, C. (2012, May). Estimating human arm's muscle force using Artificial Neural Network. In *Medical Measurements and Applications Proceedings (MeMeA), 2012 IEEE International Symposium on* (pp. 1-6). IEEE.

[26] Bueno, D. R., & Montano, L. (2013, July). Multijoint upper limb torque estimation from sEMG measurements. In *2013 35th Annual International Conference of the IEEE Engineering in Medicine and Biology Society (EMBC)* (pp. 7233-7236). IEEE.

[27] Park, J., & Lakes, R. S. (2007). *Biomaterials: an introduction*. Springer Science & Business Media.

[28] Department of Bioelectronics and Biosensors, Alagappa University. (2018). Metallic biomaterials: State of the art and new challenges. Karaikudi, Tamilnadu, India: Fundamental Biomaterials: Metals. DOI All rights reserved.

[29] Jamison, C. E., Marangoni, R. D., & Glaser, A. A. (1968). Viscoelastic properties of soft tissue by discrete model characterization. *Journal of Engineering for Industry*, *90*(2), 239-247.

[30] Snijders, C. J., Van Dijke, G. H., & Roosch, E. R. (1991). A biomechanical model for the analysis of the cervical spine in static postures. *Journal of biomechanics*, *24*(9), 783-792.

[31] Smith, S D et al. Development of a Dynamic, Deformable Finite Element Model of the Cervical Spine, *Poster No.* 798 • *ORS* 2011 *Annual Meeting*,2011

[32] del Palomar, A. P., Calvo, B., & Doblare, M. (2008). An accurate finite element model of the cervical spine under quasi-static loading. *Journal of Biomechanics*, *41*(3), 523-531.

[33] Panzer, M. B., & Cronin, D. S. (2009). C4–C5 segment finite element model development, validation, and load-sharing investigation. *Journal of biomechanics*, *42*(4), 480-490.

[34] Galbusera, F., Fantigrossi, A., Raimondi, M. T., Assietti, R., Sassi, M., & Fornari, M. (2006). Biomechanics of the C5-C6 spinal unit before and after placement of a disc prosthesis. *Biomechanics and modeling in mechanobiology*, *5*(4), 253-261.

[35] Link, H. D., McAfee, P. C., & Pimenta, L. (2004). Choosing a cervical disc replacement. *The Spine Journal*, *4*(6), S294-S302.

[36] Yoganandan, N., Kumaresan, S. C., Voo, L., Pintar, F. A., & Larson, S. J. (1996). Finite element modeling of the C4–C6 cervical spine unit. *Medical Engineering & Physics*, *18*(7), 569-574.

[37] Kode, S., Gandhi, A. A., Fredericks, D. C., Grosland, N. M., & Smucker, J. D. (2012). Effect of multilevel open-door laminoplasty and laminectomy on flexibility of the cervical spine: an experimental investigation. *Spine*, *37*(19), E1165-E1170.

[38] Makola, M. T. (2011). Cervical Spine Biomechanical Behavior and Injury.

[39] Wang, S., Song, J., Liao, Z., Feng, P., & Liu, W. (2016). Comparison of wear behaviors for an artificial cervical disc under flexion/extension and axial rotation motions. *Materials Science and Engineering: C*, *63*, 256-265.

[40] Zhao, X., Wu, Z. X., Han, B. J., Yan, Y. B., Zhang, Y., & Lei, W. (2013). Three-dimensional analysis of cervical spine segmental motion in rotation. *Archives of medical science: AMS*, *9*(3), 515.

[41] Chen, W. M., Jin, J., Park, T., Ryu, K. S., & Lee, S. J. (2018). Strain behavior of malaligned cervical spine implanted with metal-on-polyethylene, metal-on-metal, and elastomeric artificial disc prostheses–A finite element analysis. *Clinical Biomechanics*, *59*, 19-26.

[42] Corrales, M. A., & Cronin, D. S. Human Body Model Cervical Spine Curvature Effect in Extracted Motion Segment Model in Tension, Extension, and Flexion.

[43] Agah, F. (2016). *Detailed Finite Element Modeling of the Human Ligamentous Cervical Spine* (Doctoral dissertation, University of Alberta).

[44] Artificial Discs -- Surgical Fad or Real Breakthrough?. Retrieved from https://www.spineuniverse.com/treatments/emerging/artificial-discs/artificial-discs-surgical-fad-or-real-breakthrough

[45] Yeh, C. H., Hung, C. W., Kao, C. H., & Chao, C. M. (2014). Medium-term outcomes of artificial disc replacement for severe cervical disc narrowing. *Journal of Acute Disease*, *3*(4), 290-295.

[46] Chang, S. W., Bohl, M. A., Kelly, B. P., & Wade, C. (2018). The segmental distribution of cervical range of motion: A comparison of ACDF versus TDR-C. *Journal of Clinical Neuroscience*, *57*, 185-193.

[47] Diebo, B. G., Tishelman, J. C., Horn, S., Poorman, G. W., Jalai, C., Segreto, F. A., ... & Mok, J. M. (2018). The impact of mental health on patient-

reported outcomes in cervical radiculopathy or myelopathy surgery. *Journal of Clinical Neuroscience*.

[48] Burkhardt, B. W., Brielmaier, M., Schwerdtfeger, K., Sharif, S., & Oertel, J. M. (2016). Smith-Robinson procedure with an autologous iliac crest for degenerative cervical disc disease: a 28-year follow-up of 95 patients. *World neurosurgery*, *92*, 371-377.

[49] Bertagnoli, R., Duggal, N., Pickett, G. E., Wigfield, C. C., Gill, S. S., Karg, A., & Voigt, S. (2005). Cervical total disc replacement, part two: clinical results. *Orthopedic Clinics*, *36*(3), 355-362.

[50] Kibuule, L. K., & Fischgrund, J. S. (2009, September). Complications of cervical disc arthroplasty. In *Seminars in Spine Surgery* (Vol. 21, No. 3, pp. 185-193). WB Saunders.

[51] Barrett, J. (2016). *An EMG-Driven Cervical Spine Model for the Investigation of Joint Kinetics: With Application to a Helicopter Pilot Population* (Master's thesis, University of Waterloo).

[52] Galbusera, F., Bellini, C. M., Brayda-Bruno, M., & Fornari, M. (2008). Biomechanical studies on cervical total disc arthroplasty: a literature review. *Clinical Biomechanics*, *23*(9), 1095-1104.

[53] Chișiu, G., Popescu, A. M., Tudor, A., Petrescu, A. M., Stoica, G. F., & Subhi, K. A. (2018, January). Wear characteristics of UHMW polyethylene

by twist method. In *IOP Conference Series: Materials Science and Engineering* (Vol. 295, No. 1, p. 012002). IOP Publishing.

[54] EOS GmbH - Electro Optical Systems (Ed.). (2011, October). Material data sheet. Retrieved September, 2018, from www.eos.info.

[55] Golish, S. R., & Anderson, P. A. (2012). Bearing surfaces for total disc arthroplasty: metal-on-metal versus metal-on-polyethylene and other biomaterials. *The Spine Journal*, *12*(8), 693-701.

[56] Bonet, J., & Wood, R. D. (1997). *Nonlinear continuum mechanics for finite element analysis*. Cambridge university press.

[57] Panjabi, M. M., Crisco, J. J., Vasavada, A., Oda, T., Cholewicki, J., Nibu, K., & Shin, E. (2001). Mechanical properties of the human cervical spine as shown by three-dimensional load–displacement curves. *Spine*, *26*(24), 2692-2700.

[58] Wheeldon, J. A., Pintar, F. A., Knowles, S., & Yoganandan, N. (2006). Experimental flexion/extension data corridors for validation of finite element models of the young, normal cervical spine. *Journal of biomechanics*, *39*(2), 375-380.

[59] Galbusera, F., Bellini, C. M., Raimondi, M. T., Fornari, M., & Assietti, R. (2008). Cervical spine biomechanics following implantation of a disc prosthesis. *Medical engineering & physics*, *30*(9), 1127-1133.

[60] Artificial Intervertebral Disc: Cervical Spine. (2018). Retrieved from https://www.premera.com/medicalpolicies/7.01.108.pdf

[61] Cobalt Chrome Alloy Co28Cr6Mo - 3T RPD Ltd. - MAFIADOC.COM. (2018). Retrieved from https://mafiadoc.com/cobalt-chrome-alloy-co28cr6mo-3t-rpd-ltd_59fb0cff1723dd853250be59.html

[62] Cobalt Chrome Alloy Co28Cr6Mo - 3T RPD Ltd. - MAFIADOC.COM. (2018). Retrieved from https://mafiadoc.com/cobalt-chrome-alloy-co28cr6mo-3t-rpd-ltd_59fb0cff1723dd853250be59.html

[63] UHMW (Ultra-High-Molecular-Weight Polyethylene) General Material Properties. (2018). Retrieved from http://www.dielectriccorp.com/downloads/thermoplastics/uhmw.pdf

APPENDICES

Appendix A: Drawing

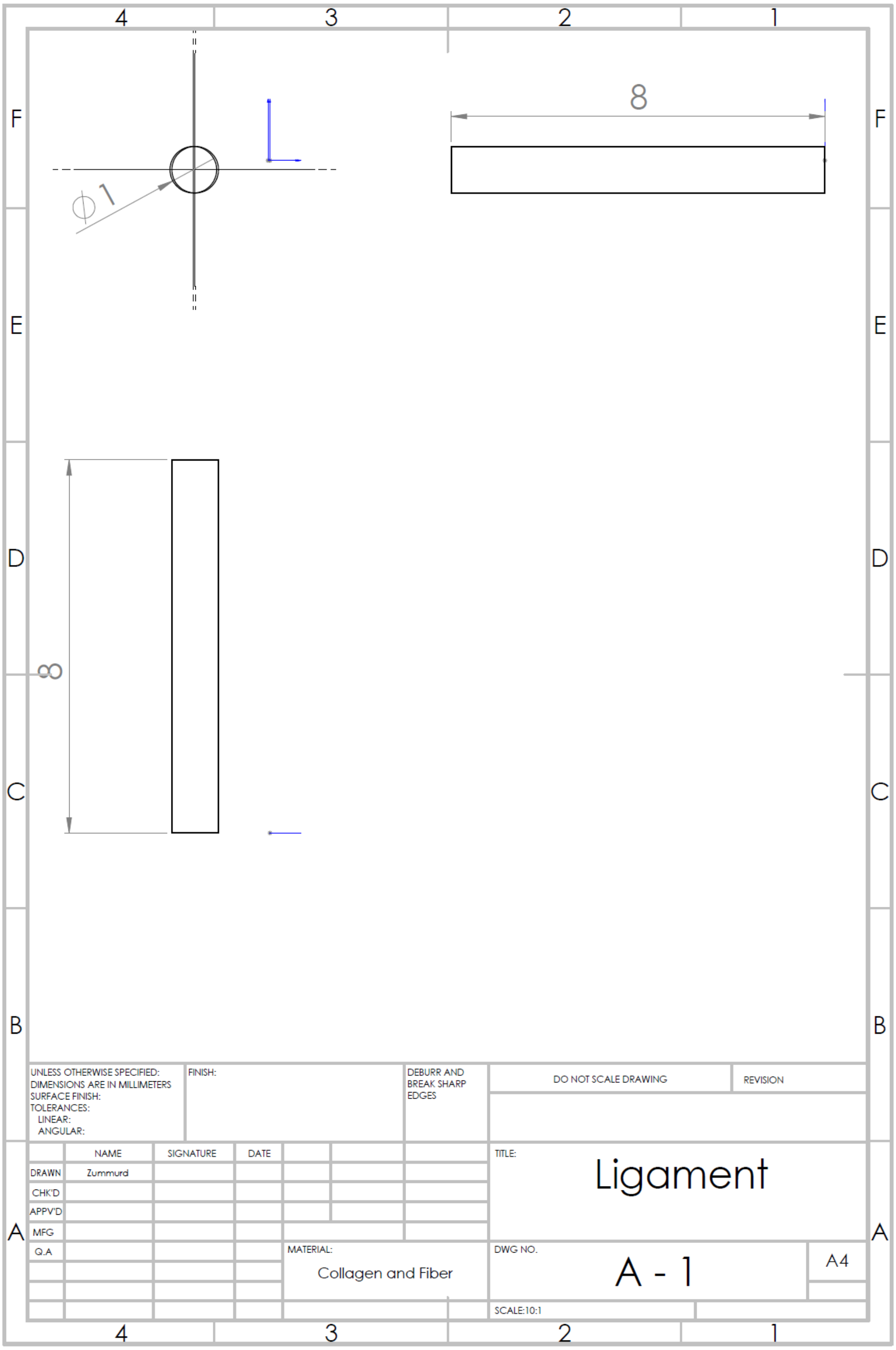

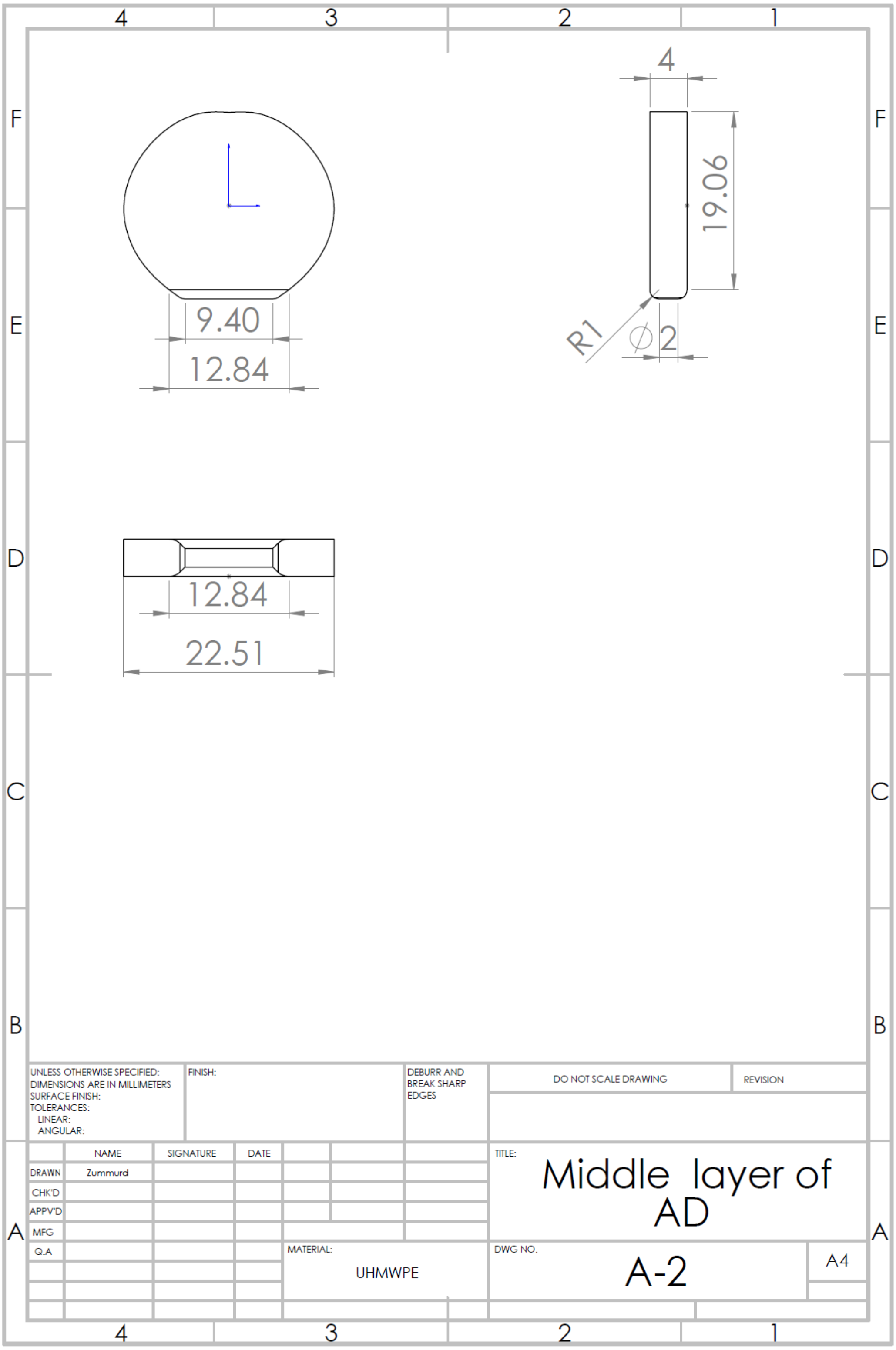
4
9.40
12.84
12.84
22.51
19.06
R1
∅2
UNLESS OTHERWISE SPECIFIED:
DIMENSIONS ARE IN MILLIMETERS
SURFACE FINISH:
TOLERANCES:
LINEAR:
ANGULAR:
FINISH:
DEBURR AND BREAK SHARP EDGES
DO NOT SCALE DRAWING
REVISION
NAME
SIGNATURE
DATE
DRAWN
Zummurd
CHK'D
APPV'D
MFG
Q.A
TITLE:
Middle layer of AD
MATERIAL:
UHMWPE
DWG NO.
A-2
A4

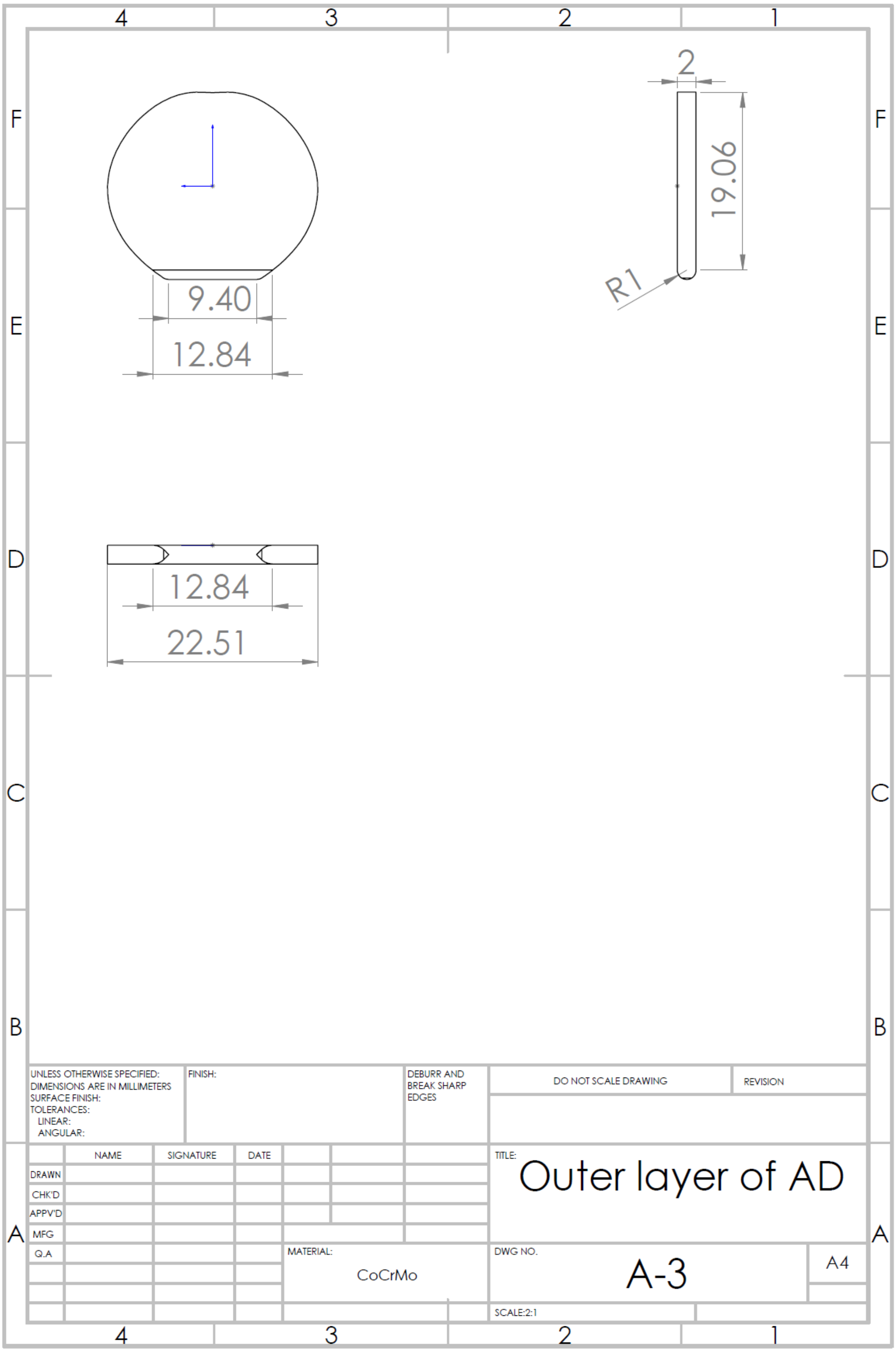

9.40
12.84
2
19.06
R1
12.84
22.51
UNLESS OTHERWISE SPECIFIED:
DIMENSIONS ARE IN MILLIMETERS
SURFACE FINISH:
TOLERANCES:
LINEAR:
ANGULAR:
FINISH:
DEBURR AND BREAK SHARP EDGES
DO NOT SCALE DRAWING
REVISION
NAME
SIGNATURE
DATE
DRAWN
CHK'D
APPV'D
MFG
Q.A
TITLE:
Outer layer of AD
MATERIAL:
CoCrMo
DWG NO.
A-3
A4
SCALE:2:1

Appendix B: ABAQUS Report

The Abaqus Software is a product of:

P R O B L E M   S I Z E

NUMBER OF ELEMENTS IS 26482

NUMBER OF NODES IS 39423

NUMBER OF NODES DEFINED BY THE USER 39423

TOTAL NUMBER OF VARIABLES IN THE MODEL 119940

(DEGREES OF FREEDOM PLUS MAX NO. OF ANY LAGRANGE MULTIPLIER

VARIABLES. INCLUDE *PRINT,SOLVE=YES TO GET THE ACTUAL NUMBER.)

END OF USER INPUT PROCESSING

JOB TIME SUMMARY

USER TIME (SEC) = 2.3000

SYSTEM TIME (SEC) = 0.20000

TOTAL CPU TIME (SEC) = 2.5000

WALLCLOCK TIME (SEC) = 3

1

Abaqus 6.12-1 Date 20-Dec-2018 Time 06:31:33

For use by under license from Dassault Systemes or its subsidiary.

STEP 1 INCREMENT 1

TIME COMPLETED IN THIS STEP 0.00

S T E P   1   S T A T I C   A N A L Y S I S

AUTOMATIC TIME CONTROL WITH -

A SUGGESTED INITIAL TIME INCREMENT OF 1.000E-03

AND A TOTAL TIME PERIOD OF 50.0

THE MINIMUM TIME INCREMENT ALLOWED IS 1.000E-05

THE MAXIMUM TIME INCREMENT ALLOWED IS 1.00

LINEAR EQUATION SOLVER TYPE DIRECT SPARSE

LARGE DISPLACEMENT THEORY WILL BE USED

M E M O R Y   E S T I M A T E

PROCESS FLOATING PT MINIMUM MEMORY MEMORY TO

OPERATIONS REQUIRED MINIMIZE I/O

PER ITERATION (MBYTES) (MBYTES)

1 2.96E+011 236 1795

E L E M E N T Q U A L I T Y C H E C K S

P R O B L E M S I Z E

NUMBER OF ELEMENTS IS 26482

NUMBER OF NODES IS 39423

NUMBER OF NODES DEFINED BY THE USER 39423

TOTAL NUMBER OF VARIABLES IN THE MODEL 119940

(DEGREES OF FREEDOM PLUS MAX NO. OF ANY LAGRANGE MULTIPLIER

VARIABLES. INCLUDE *PRINT,SOLVE=YES TO GET THE ACTUAL NUMBER.)

END OF USER INPUT PROCESSING

JOB TIME SUMMARY

USER TIME (SEC) = 2.4000

SYSTEM TIME (SEC) = 0.30000

TOTAL CPU TIME (SEC) = 2.7000

WALLCLOCK TIME (SEC) = 3

1

Abaqus 6.12-1 Date 20-Dec-2018 Time 15:18:10

For use by under license from Dassault Systemes or its subsidiary.

STEP 1 INCREMENT 1

TIME COMPLETED IN THIS STEP 0.00

S T E P 1 S T A T I C A N A L Y S I S

AUTOMATIC TIME CONTROL WITH -

A SUGGESTED INITIAL TIME INCREMENT OF 1.000E-05

AND A TOTAL TIME PERIOD OF 120.

THE MINIMUM TIME INCREMENT ALLOWED IS 1.000E-08

THE MAXIMUM TIME INCREMENT ALLOWED IS 1.00

LINEAR EQUATION SOLVER TYPE DIRECT SPARSE

LARGE DISPLACEMENT THEORY WILL BE USED

M E M O R Y E S T I M A T E

PROCESS	FLOATING PT OPERATIONS PER ITERATION	MINIMUM MEMORY REQUIRED (MBYTES)	MEMORY TO MINIMIZE I/O (MBYTES)
1	2.96E+011	236	1795

THE ANALYSIS HAS BEEN COMPLETED

ANALYSIS COMPLETE

WITH 73 WARNING MESSAGES ON THE DAT FILE

JOB TIME SUMMARY

USER TIME (SEC) = 6321.2

SYSTEM TIME (SEC) = 63.800

TOTAL CPU TIME (SEC) = 6385.0

WALLCLOCK TIME (SEC) = 6399

S T E P 1 C A L C U L A T I O N O F E I G E N V A L U E S

F O R N A T U R A L F R E Q U E N C I E S

THE LANCZOS EIGENSOLVER IS USED FOR THIS ANALYSIS

Abaqus WILL COMPUTE UNCOUPLED

STRUCTURAL AND ACOUSTIC MODES

NUMBER OF EIGENVALUES 20

HIGHEST FREQUENCY OF INTEREST 1.00000E+18

MAXIMUM NUMBER OF STEPS WITHIN RUN 35

BLOCK SIZE FOR LANCZOS PROCEDURE 7

THE EIGENVECTORS ARE SCALED SO THAT

THE LARGEST DISPLACEMENT ENTRY IN EACH VECTOR

IS UNITY

THIS IS A LINEAR PERTURBATION STEP.

ALL LOADS ARE DEFINED AS CHANGE IN LOAD TO THE REFERENCE STATE

TOTAL MASS OF MODEL

3.9593612E-02

LOCATION OF THE CENTER OF MASS OF THE MODEL

-0.1339890 -1.595049 -1.999998

MOMENTS OF INERTIA ABOUT THE ORIGIN

I(XX)	I(YY)	I(ZZ)
5.069232	5.238367	3.896099

PRODUCTS OF INERTIA ABOUT THE ORIGIN

I(XY)	I(XZ)	I(YZ)
-1.1457477E-02	-1.0610183E-02	-0.1263069

MOMENTS OF INERTIA ABOUT THE CENTER OF MASS

I(XX) I(YY) I(ZZ)

4.810124 5.079282 3.794655

PRODUCTS OF INERTIA ABOUT THE CENTER OF MASS

I(XY)	I(XZ)	I(YZ)
-2.9955729E-03	2.2425105E-08	4.8895765E-07

M E M O R Y E S T I M A T E

PROCESS	FLOATING PT OPERATIONS PER ITERATION	MINIMUM MEMORY REQUIRED (MBYTES)	MEMORY TO MINIMIZE I/O (MBYTES)
1	2.96E+011	239	2719

E I G E N V A L U E O U T P U T

MODE NO	EIGENVALUE	FREQUENCY (RAD/TIME)	(CYCLES/TIME)	GENERALIZED MASS	COMPOSITE MODAL DAMPING
1	1.26919E+06	1126.6	179.30	1.19643E-02	0.0000
2	1.57199E+06	1253.8	199.55	3.38389E-03	0.0000
3	2.58059E+06	1606.4	255.67	6.72891E-04	0.0000
4	4.00423E+06	2001.1	318.48	7.11109E-05	0.0000
5	4.04392E+06	2010.9	320.05	1.53874E-04	0.0000
6	4.04712E+06	2011.7	320.18	8.82072E-05	0.0000
7	4.88073E+06	2209.2	351.61	1.62412E-04	0.0000
8	9.01882E+06	3003.1	477.96	2.54408E-03	0.0000
9	1.09186E+07	3304.3	525.90	9.39218E-04	0.0000
10	1.31042E+07	3620.0	576.14	2.11827E-03	0.0000
11	1.34050E+07	3661.3	582.71	4.31138E-03	0.0000
12	1.34050E+07	3661.3	582.71	4.35129E-03	0.0000
13	1.34066E+07	3661.5	582.75	4.62327E-03	0.0000
14	1.34067E+07	3661.5	582.75	4.60693E-03	0.0000
15	1.34068E+07	3661.5	582.75	5.58361E-03	0.0000

P A R T I C I P A T I O N F A C T O R S

MODE NO	X-COMPONENT	Y-COMPONENT	Z-COMPONENT	X-ROTATION	Y-ROTATION	Z-ROTATION
1	7.41251E-03	1.4263	-5.37438E-02	14.665	-8.99419E-02	-0.22584
2	2.6467	-1.00319E-02	-2.89302E-03	-0.12365	-26.613	10.752
3	-1.5388	5.28709E-02	1.04763E-02	-6.42094E-05	16.058	58.113
4	1.8004	0.34966	7.95040E-02	-13.506	9.0350	28.679
5	-0.88219	0.26378	5.29032E-02	-0.60172	-4.5821	-11.986

6	1.2408	-0.19381	-4.99964E-02	14.185	6.2392	21.937
7	0.26415	-7.15453E-02	-1.61416E-02	0.50659	8.4029	-46.931
8	9.23724E-02	1.6350	1.9827	-17.003	1.1604	-0.25977
9	3.0668	-0.23854	0.14628	2.3295	35.215	3.4412
10	0.13135	1.1809	-3.2429	-9.6911	1.2477	-3.83024E-03
11	-7.06952E-04	-3.94761E-03	1.18985E-02	3.07304E-02	-9.65698E-03	-2.01683E-04
12	1.31842E-03	4.71418E-04	-2.50206E-03	-1.80178E-03	1.65686E-02	1.93594E-03
13	3.28337E-04	-1.51110E-03	2.45142E-03	1.17415E-02	1.20917E-02	5.62746E-03
14	4.31929E-03	-1.86442E-03	3.90325E-03	1.72497E-02	5.63665E-02	4.72132E-03
15	2.93253E-04	1.83414E-03	-5.19413E-03	-1.52974E-02	1.96631E-03	2.68557E-04

E F F E C T I V E M A S S

MODE NO	X-COMPONENT	Y-COMPONENT	Z-COMPONENT	X-ROTATION	Y-ROTATION	Z-ROTATION
1	6.57383E-07	2.43409E-02	3.45576E-05	2.5732	9.67859E-05	6.10249E-04
2	2.37041E-02	3.40553E-07	2.83218E-08	5.17360E-05	2.3966	0.39119
3	1.59326E-03	1.88095E-06	7.38521E-08	2.77423E-12	0.17350	2.2724
4	2.30494E-04	8.69407E-06	4.49484E-07	1.29721E-02	5.80485E-03	5.84874E-02
5	1.19753E-04	1.07068E-05	4.30654E-07	5.57121E-05	3.23063E-03	2.21078E-02
6	1.35805E-04	3.31332E-06	2.20486E-07	1.77495E-02	3.43370E-03	4.24467E-02
7	1.13327E-05	8.31343E-07	4.23166E-08	4.16800E-05	1.14677E-02	0.35771
8	2.17078E-05	6.80116E-03	1.00009E-02	0.73552	3.42541E-03	1.71676E-04
9	8.83356E-03	5.34437E-05	2.00961E-05	5.09692E-03	1.1647	1.11224E-02
10	3.65482E-05	2.95409E-03	2.22772E-02	0.19894	3.29751E-03	3.10766E-08
11	2.15475E-09	6.71871E-08	6.10377E-07	4.07148E-06	4.02068E-07	1.75370E-10
12	7.56352E-09	9.67008E-10	2.72403E-08	1.41261E-08	1.19452E-06	1.63080E-08
13	4.98413E-10	1.05569E-08	2.77834E-08	6.37374E-07	6.75966E-07	1.46411E-07
14	8.59482E-08	1.60140E-08	7.01882E-08	1.37080E-06	1.46371E-05	1.02693E-07
15	4.80176E-10	1.87836E-08	1.50640E-07	1.30663E-06	2.15883E-08	4.02705E-10
TOTAL	3.46873E-02	3.41755E-02	3.23349E-02	3.5436	3.7656	3.1563

1

Abaqus 6.12-1 Date 23-Dec-2018 Time 18:05:26

STEP 2 INCREMENT 1

TIME COMPLETED IN THIS STEP 0.00

S T E P 2 S T E A D Y S T A T E A N A L Y S I S

FULL STRUCTURAL-ACOUSTIC COUPLING IS USED IN THIS

FORCED RESPONSE ANALYSIS

FREQUENCY RANGE DEFINITIONS (CYCLES/TIME)

LOW	HIGH	POINTS	BIAS	SCALE FACTOR	TYPE OF SCALING
1.00	520.	20	3.00	1.00	Logarithmic

INTERVAL WILL BE DIVIDED FIRST USING EIGENFREQUENCIES

THIS IS A LINEAR PERTURBATION STEP.

ALL LOADS ARE DEFINED AS CHANGE IN LOAD TO THE REFERENCE STATE

M E M O R Y   E S T I M A T E

PROCESS	FLOATING PT OPERATIONS PER ITERATION	MINIMUM MEMORY REQUIRED (MBYTES)	MEMORY TO MINIMIZE I/O (MBYTES)
1	0.00E+000	59	1282

INCREMENT NUMBER 1

FREQUENCY = 1.0000000

INCREMENT NUMBER 2

FREQUENCY = 1.0990339

INCREMENT NUMBER 3

FREQUENCY = 1.2172478

INCREMENT NUMBER 4

FREQUENCY = 1.3610952

INCREMENT NUMBER 171

FREQUENCY = 519.20294

INCREMENT NUMBER 172

FREQUENCY = 520.00000

THE ANALYSIS HAS BEEN COMPLETED

ANALYSIS COMPLETE

WITH 63 WARNING MESSAGES ON THE DAT FILE

JOB TIME SUMMARY

USER TIME (SEC) = 121.70

SYSTEM TIME (SEC) = 9.6000

TOTAL CPU TIME (SEC) = 131.30

WALLCLOCK TIME (SEC) = 135

Appendix C: Medical Standards

Table 6: Policy Coverage Criteria

Site of Service for Elective Surgical Procedures	Medical Necessity
Medically necessary sites of service: **Off campus-outpatient hospital/medical center** **On campus-outpatient hospital/medical center** **Ambulatory Surgical Center**	Certain elective surgical procedures will be covered in the most appropriate, safe, and cost effective site. These are the preferred medically necessary sites of service for certain elective surgical procedures.
Inpatient hospital/medical center	**Certain elective surgical procedures will be covered in the most appropriate, safe, and cost-effective site. This site is considered medically necessary only when the patient has a clinical condition which puts him or her at increased risk for complications including any of the following (this list may not be all inclusive):** • Anesthesia Risk • ASA classification III or higher (see **definition**) • Personal history of complication of anesthesia • Documentation of alcohol dependence or history of cocaine use • Prolonged surgery (>3 hours) • Cardiovascular Risk • Uncompensated chronic heart failure (**NYHA class** III or IV) • Recent history of myocardial infarction (MI) (<3 months) • Poorly controlled, resistant hypertension***** • Recent history of cerebrovascular accident (< 3 months) • Increased risk for cardiac ischemia (drug eluting stent placed < 1 year or angioplasty <90 days) • Symptomatic cardiac arrhythmia despite medication • Significant valvular heart disease Liver Risk • Advance liver disease (MELD Score > 8)****** Pulmonary Risk • Chronic obstructive pulmonary disease (COPD) (FEV1<50%) • Poorly controlled asthma (FEV1 <80% despite treatment) • Moderate to severe obstructive sleep apnea (OSA)******* Renal Risk • End stage renal disease (on dialysis) Other • Morbid obesity (BMI ≥ 50)

	• Pregnancy • Bleeding disorder (requiring replacement factor, blood products, or special infusion product [DDAVP**** does not meet this criteria]) • Anticipated need for transfusion(s) * 3 or more drugs to control blood pressure ** https://reference.medscape.com/calculator/meld-score-end-stage-liverdisease *** Moderate-AHI≥15 and ≤ 30, Severe-AHI ≥30 ****DDAVP-Deamino-Delta-D-Arginine Vasopressin (Desmopressin)
Inpatient hospital/medical center	**This site of service is considered NOT medically necessary for** **certain elective surgical procedures when the site of service** **criteria listed above are not met.**

Surgery	Medical Necessity
Artificial cervical intervertebral disc implantation	**Implanting an artificial cervical intervertebral disc may be** **considered medically necessary when ALL of the following** **criteria are met:** • The device is approved by Food and Drug Administration (FDA): o For one level: • Bryan® Cervical Disc (Medtronic) • Mobi-C® (LDR Medical) • PCM (porous-coated motion) Cervical Disc® (NuVasive) • Prestige® Cervical Disc System (Medtronic) • ProDisc-C® Total Disc Replacement (DePuySynthes) • SECURE-C® Cervical Artificial Disc (Globus Medical) o For two contiguous levels: • Mobi-C Cervical Disc Prosthesis • Prestige LP Cervical Disc • The patient is skeletally mature • The patient has intractable cervical radicular pain or myelopathy a. Which has failed at least 6 weeks of conservative nonoperative treatment including physical therapy and at least one of the following: • Acupuncture • Cervical collar • Corticosteroids • Exercise program • Medical treatment with NSAIDs or other analgesics **OR** b. The patient has severe or rapidly progressive

	symptoms of nerve root or spinal cord compression requiring hospitalization or immediate surgical treatment. • Degeneration is documented by imaging within the prior 12 months (magnetic resonance imaging, computed tomography or myelography) • Cervical degenerative disc disease is from C3 through C7 • The patient is free from contraindication to artificial cervical intervertebral disc implantation
Subsequent artificial cervical intervertebral disc implantation	**Subsequent implantation of a second artificial cervical intervertebral disc at an adjacent level (contiguous to a previous placed artificial disc)may be considered medically necessary if the above criteria are met for each disc level, and the device is FDA-approved for 2 levels (eg, Mobi-C, Prestige LP) and the initial cervical artificial disc implantation is fully healed.**

Surgery	**Investigational**
Artificial cervical intervertebral disc implantation	**Implantation of an artificial cervical intervertebral disc is considered investigational for all other indications, including the following:** Active infection Anatomical deformity (eg, ankylosing spondylitis) Combined use of an artificial cervical disc and fusion (hybrid surgery) Disc implantation at more than 2 levels Malignancy Metabolic bone disease (eg, osteoporosis, osteopenia, osteomalacia) Presence of facet arthritis Previous fusion at another cervical level Prior surgery at the treated level Rheumatoid arthritis or other autoimmune disease Translational instability

Documentation Requirements
The following information must be submitted to ensure an accurate, expeditious, and complete review for cervical spinal fusion surgery: Specific procedures requested with related procedure/diagnosis codes and identification of disc level(s) for surgery and device to be implanted Clinical notes that include a current history and physical exam Clinical notes that document the requesting surgeon personally evaluated the individual at least twice before submitting a request for surgery (except in cases of malignancy, trauma, infection or rapidly progressive neurologic symptoms) Detailed documentation of extent and response to non-operative conservative therapy, if applicable, including outcomes of any procedural interventions, medications used and physical therapy/physiatrist notes Copy of radiologist's report(s) for diagnostic imaging (MRIs, CTs, etc.) completed within the past 12 months. Imaging must be performed and read by an independent radiologist. If discrepancies should arise in the interpretation of the imaging, the radiologist's report will supersede.

Table 7: Coding

Code	Description
CPT	
0095T	Removal of total disc arthroplasty (artificial disc), anterior approach, each additional interspace; cervical
0098T	Revision including replacement of total disc arthroplasty (artificial disc), anterior approach, each additional interspace; cervical
0375T	Total disc arthroplasty (artificial disc), anterior approach, including discectomy with end plate preparation (includes osteophytectomy for nerve root or spinal cord decompression and microdissection), cervical, three or more levels
22856	Total disc arthroplasty (artificial disc), anterior approach, including discectomy with end plate preparation (includes osteophytectomy for nerve root or spinal cord decompression and microdissection); single interspace, cervical
22858	Total disc arthroplasty (artificial disc), anterior approach, including discectomy with end plate preparation (includes osteophytectomy for nerve root or spinal corddecompression and microdissection; second level, cervical
22861	Revision including replacement of total disc arthroplasty (artificial disc), anterior approach, single interspace; cervical
22864	Removal of total disc arthroplasty (artificial disc), anterior approach, single interspace; cervical

Cervical Disc Prostheses under investigation in the United States

Prosthesis	Manufacturer	FDA Status
Kineflex C	Spinal Motion	FDA IDE trial complete; status unknown
Freedom	AxioMed	FDA IDE trial recruiting
M6-C	Spinal Kinetics	FDA IDE trial recruiting

		complete

FDA: U.S. Food and Drug Administration; IDE: investigational device exemption

This appendix is adopted from [61]

Appendix D: Engineering Standard

Table 8: Cobalt Chrome Alloy Co28Cr6Mo

Technical Data:		
Minimum recommended Layer Thickness:	20 µm	
Minimum Wall Thickness:	0.4mm	
Volume Rate:	between 1.6-3 mm3/s	
Physical and Chemical Properties:		
Relative Density with Standard Parameters	approx. 100% (8.29 g/cm3)	
Material composition	Co 60-65 wt% Si max 1 w% C max 0.16 wt% Cr 26-30 wt% Mn max1 wt% Ni max 1 wt% Mo 5-7 wt% Fe max 0.75 wt%	
Mechanical Properties at 20 ^{o}C:		
Ultimate Tensile Strength (MPIF 10 -horizontal direction (XY) - vertical direction (Z)	1300 MPa ± 50 MPa 1150 MPa ± 50 MPa	
Yield strength (Rp 0.2%) - horizontal direction (XY) - vertical direction (Z)	980 MPa ± 50 MPa 880 MPa ± 50 MPa	
Elongation at break - horizontal direction (XY) - vertical direction (Z) - after HIPping	11% + 2% 9% + 1% 21-24%	
Young's Modulus - horizontal direction (XY) - vertical direction (Z)	220 GPa ± 20 GPa 220 GPa ± 20 GPa	
Fatigue life* - in vertical direction (Z) at 0-400 MPa load range and 20Hz	approx. 7.2 million cycles	
Hardness (DIN EN ISO 6508-1)	40-45 HRC	
Surface roughness - after shot-peening - after polishing	approx. Ra 10 µm Rz up to < 1 µm	
Thermal Properties:		
Coefficient of Thermal Expansion	over 20-500oC 13.6 x 10-6 m/moC	over 500-1000oC 15.1 x 10-6 m/moC
Thermal conductivity	- at 20oC 13 W/moC - at 300oC 18 W/moC	- at 500oC 22 W/moC - at 1000oC 33W/moC
Maximum operating temperature	1150oC	
Melting range	1350-1430oC	

ISO 9001:2008 & ISO 13485:2003 Medical Devices certifications

AS 9100 Rev C for the production of metal parts using Additive Manufacturing (AM)

Table 9: UHMWPE

General	
Density	931 - 949 kg/m^3
Yield Strength	2.14e7 - 2.76e7 Pa
Tensile Strength	3.86e7 - 4.83e7 Pa

Elongation	3.5 -5.25 % strain
Hardness (Vickers)	6.28e7 - 8.14e7 Pa
Impact Strength (notched)	9.52e4 - 1.05e5 J/m^2
Fracture Toughness	1.72e6 - 5.16e6 Pa/m^0.5
Young's Modulus	8.94e8 - 9.63e8 Pa
Thermal	
Max Service Temperature	110 - 130 °C
Melting Temperature	125 - 138
Insulator or Conductor	Insulator
Specific Heat Capability	1.75e3 - 1.81e3 J/kg °C
Thermal Expansion Coefficent	2.34e-4 - 3.6e-4 strain/°C
Eco	
CO2 Footprint	3.16 - 3.49 kg/kg
Recycleable	Yes

This appendix adopted from [62, 63]